




Novel Approach for Transdermal Delivery of Rifampicin to Induce Synergistic Antimycobacterial Effects Against Cutaneous and Systemic Tuberculosis Using a Cationic Nanoemulsion Gel

This article was published in the following Dove Press journal:
International Journal of Nanomedicine

Afzal Hussain ¹
Mohammad A Altamimi¹
Sultan Alshehri¹
Syed Sarim Imam ¹
Faiyaz Shakeel ¹
Sandeep Kumar Singh²

¹Department of Pharmaceutics, College of Pharmacy, King Saud University, Riyadh, Kingdom of Saudi Arabia;

²Department of Pharmaceutical Sciences, Birla Institute of Technology, Ranchi, Jharkhand, India

Purpose: This study demonstrated improved transdermal delivery of rifampicin-loaded cationic nanoemulsion gel to treat systemic and cutaneous tuberculosis using capmul, labrasol, and acconon, which exert anti-*Mycobacterium* activities. This approach enhanced drug permeation across the skin, increased therapeutic efficacy, and reduced dose-related side effects.

Methods: Design Expert[®] was used to optimize formulations (S_{mix} ratio and capmul as independent factors), which were prepared using a slow spontaneous titration method. The optimized nanoemulsion was incorporated into carbopol gel to allow for topical application and comparative assessments. Nanoemulsions and gels were evaluated for size, size distribution, shape, zeta potential, percent spread, viscosity, in vitro hemolysis, in vitro release, and ex vivo skin permeation and deposition. A mechanistic evaluation was performed using scanning electron microscopy. Furthermore, in vivo pharmacokinetic and irritation studies were performed.

Results: The optimized cationic nanoemulsion (OCNE-1) was characterized by small particle size (≤ 100 nm), had optimal viscosity, percent spread, zeta potential, and percent drug release, and was hemocompatible. The OCNE-1T gel exhibited higher permeation flux ($51.32 \pm 0.5 \mu\text{g}/\text{cm}^2 \text{ hr}$), permeation coefficient ($2.566 \pm 0.08 \text{ cm/hr}$), drug deposition ($994.404 \mu\text{g}/\text{cm}^2$), and enhancement ratio (7.16) than those of the OCNE-1 nanoemulsion or drug solution. Scanning electron microscopy was used to characterize the mechanism of enhanced permeation. An in vivo study showed that the C_{max} and area under the curve following transdermal application were 4.34- and 4.74-fold higher than those following oral administration.

Conclusion: Transdermal delivery of rifampicin could be a promising alternative to conventional approaches to treat systemic and local tuberculosis, and other bacterial infections.

Keywords: systemic and cutaneous tuberculosis, nanoemulsion gel, transdermal delivery, permeation parameters, bioavailability

Introduction

Tuberculosis (TB) is the most widespread airborne disease caused by the *Mycobacterium tuberculosis*. The global tuberculosis report of the World Health Organization (WHO) estimated that 10.0 million tuberculosis cases occurred in 2019 globally, and BRICS (Brazil, Russia, India, China, and South Africa) accounted for 47% of the total number of reported TB cases.¹ Cutaneous tuberculosis spans a wide spectrum (tuberculosis cutis orificialis, Lupus vulgaris, scrofuloderma, and

Correspondence: Afzal Hussain
Department of Pharmaceutics, College of Pharmacy, King Saud University, P.O. Box 2457, Riyadh 11451, Kingdom of Saudi Arabia
Tel +966 5 64591584
Email afzal.pharma@gmail.com

tuberculosis verrucosa cutis), and the manifestation depends on host cell-mediated immunity.²⁻⁴ Skin microflora normally consist of *Staphylococcus* spp., *Propionibacterium* spp., *Corynebacterium* spp., *Malassezia* spp., *Candida* spp., *Debaryomyces*, and *Cryptococcus* spp. These adhere, invade and multiply for pathogenesis.⁵ Rifampicin (RIF), a lipophilic drug, does not easily penetrate bacterial cell walls. Formulation of RIF in a self-emulsifying drug delivery system comprised of salicylic acid and benzoic acid has been shown to be effective against bacterial and fungal infections.⁶ Moreover, RIF-loaded niosomes have been reported as a topical treatment for acne.⁷ Rifampicin is a wide spectrum antibiotic against *Mycobacterium* and gram-positive bacteria at low concentrations.⁸ Rifampicin is unstable at acidic pH, which results in limited oral absorption, stability, and bioavailability. Therefore, RIF has been included in nanoemulsions for parenteral administration.⁹

Oral administration of drugs often results in poor patient compliance due to limited aqueous solubility and adverse effects. Oral administration of isoniazid (INH; a potential anti-tuberculosis drug used as monotherapy for latent tuberculosis) is effective, but compliance is poor due to hepatotoxicity and peripheral neuropathy.¹⁰ Transdermal delivery of molecules with poor solubility or bioavailability has been evaluated as an alternative method to oral or parenteral administration.¹¹ Transdermal delivery results in several benefits such as sustained and controlled drug release, reduced fluctuation of plasma drug concentration, improved control of cutaneous infection, elimination of the hepatic first-pass effect, high patient compliance, reduced doses and dose-associated side effects, and this route of administration is non-invasive. Previous studies evaluated the transdermal delivery of INH/RIF and reported avoidance of the hepatic first-pass effect, which resulted in dose reduction and mitigation of side effects (peripheral neuropathy and hepatotoxicity).^{10,12} Chen et al investigated transdermal delivery of RIF and INH using electro-phonophoresis for treatment of superficial skin tuberculosis and tubercular lymphadenitis.¹² However, these drugs were evaluated as components of a nanocarrier-based transdermal delivery system.

Rifampicin (Log P ~ 3.8) is the first-line treatment for pulmonary and tubercular lymphadenitis (cutaneous tuberculosis).¹² However, RIF has limited aqueous solubility (~1 mg/mL) and is a Class II drug according to the Biopharmaceutical Classification System. Therefore, RIF may be a promising candidate for augmented transdermal delivery using isotropic and thermodynamically stable

nanoemulsions comprised of excipients that have innate anti-*Mycobacterium* activity.¹³⁻¹⁵ Ethanol, menthol, limonene, and Transcutol have been shown to enhance the permeation of INH. Transcutol (5% w/v) exhibited reduced skin partitioning (flux) of hydrophilic INH across the pig skin which indicated that it may be a good permeation enhancer for hydrophobic molecules such as RIF.¹⁰ Previous studies have shown that Transcutol-HP enhanced penetration of amphotericin B, which is lipophilic. This may have resulted from alcohol-mediated solubilization of the drug in the lipophilic domain of the stratum corneum (SC).¹⁴ The SC is a well-characterized keratinized crystalline barrier against several substances (foreign particles or molecules), particularly hydrophilic drugs. Moreover, the SC augments the transdermal delivery of lipophilic drugs.^{12,14}

In our previous studies, excipients with innate activity against virulent and non-virulent strains of *Mycobacterium* were loaded with RIF in self-emulsifying formulations. These formulations exhibited improved dissolution rates and in vivo pharmacokinetic parameters following oral delivery.^{15,16} The present study has focussed on transdermal delivery of RIF-loaded cationic nanoemulsion gels comprised of excipients (lipids and surfactants) with anti-*Mycobacterium* activity for the treatment of cutaneous tuberculosis and systemic infection. This study evaluated the effects of labrasol (LAB) and capmul PG8 (CPG8) on permeation parameters (permeation flux, drug deposition, and permeation coefficient). In addition, the mechanisms of enhanced permeation were evaluated using scanning electron microscopy (SEM). Finally, in vivo studies were performed to demonstrate improved bioavailability and reduced irritation resulting from the administration of the developed formulation in rats.

Materials and Methods

Materials

Rifampicin (97.0% pure) was provided *ex gratia* by Unicare India Pvt. Ltd. (New Delhi, India). Capmul PG8 NF (propylene glycol monoester of caprylic acid) was purchased from Abitec (USA). Tween[®] 80 was purchased from Merck Chemicals Mumbai, India. Transcutol-HP and labrasol (LAB) were gifted by Gattefossé (36 chem de Genas-BP 603-F-69804 Saint Priest Cedex France). Rifampicin for injection (USP; containing 10 mg of inert sodium formaldehyde sulfoxide and sodium hydroxide to adjust pH; 60 mg/mL) was purchased from a local pharmacy for use as a drug solution (DS). An ultra-performance liquid chromatography (UPLC)

system (Thermo Scientific, City, USA) equipped with a C18 column (Purospher Star RP-18 HPLC cartridge column; 50 mm× 4.6 mm, internal diameter, 3- μ m particle size of stationary packing in column; Merck, Germany) and a rotary vacuum pump (E2M30, Edwards High Vacuum International, West Sussex, UK) were used for analytical procedures. All chemicals (including solvents) used in this study were of analytical grade.

Non-virulent strains (MTTC 995 and MTTC 942) were procured from microbial type culture collection, IIMTECH (Indian Institute of Microbial Technology, Chandigarh) Punjab, India, and revived in our laboratory. The experimental strain *Mycobacterium tuberculosis H₃₇ Rv* (ATCC 25618) (not cultured in our lab) was used to study the susceptibility test at Itki, Ranchi, Jharkhand India.¹⁵

Methods

Screening of Excipients

Solubility Assessment of RIF in Excipients

Lipids, surfactants, and co-surfactants (Table 1) were used to solubilize RIF as previously described.¹⁶ This experiment was performed at 40 °C until saturation was achieved. Excess RIF was added to vials containing 3 mL of each individual excipient to determine saturation solubility. To promote facilitated solubilization, samples were placed in an isothermal water bath shaker (Remi Equipment Pvt. Ltd., Mumbai, India) at 40 ± 1 °C for 40 hrs. After reaching equilibrium, the samples were centrifuged to remove undissolved RIF. The supernatant was diluted with methanol, and dissolved content was

measured using a UV/Vis spectrophotometer at λ_{max} 337 nm (Shimadzu, U-1800, Tokyo, Japan).

In vitro Anti-Mycobacterium Activities

Excipients (lipid, surfactant, and co-surfactant) were screened for inclusion in nanoemulsions in vitro by performing anti-*Mycobacterium* studies using non-virulent strains (*Mycobacterium smegmatis*, MS-995 and *Mycobacterium smegmatis*, MS-942) and the clinical experimental strain *Mycobacterium tuberculosis H₃₇ Rv* (IRL, Itki, Ranchi, India), as previously reported.¹⁵ The strains (MS-995 and MS-942) were cultured until they reached the logarithmic growth phase (OD₆₀₀ ~ 0.6) in sterilized (121°C for 15 min) nutrient broth at 37 ± 1°C and pH 7.0, then diluted in with nutrient broth (2.5 × 10⁷ CFU/mL of MS-995 and 1.8 × 10⁷ CFU/mL of MS-942). The culture suspension (1 mL) and sterilized nutrient agar media (25 mL) were combined in petri dishes at room temperature. The mixed contents were allowed to solidify, and wells were made using a sterilized stainless-steel borer (8-mm in diameter). The test sample was poured into the well and incubated for 24 hrs. The zone of inhibition around the well was measured. To determine MIC value (minimum inhibitory concentration), 1 mL of culture, 1 mL of test sample, and 25 mL of sterilized nutrient agar were mixed at room temperature then solidified and incubated for 24 hrs. Activity was expressed in terms of MIC value and defined as the minimum concentration at

Table 1 Selection of Excipients Based on the Solubility of RIF and Anti-*Mycobacterium* Activities of Various Lipids and Surfactants

| Excipients | HLB | Solubility (mg/mL) | Anti- <i>Mycobacterium</i> Activities | | |
|-------------------------|-------|--------------------|---------------------------------------|----------------------|--|
| | | | MIC (MS-995) (mg/mL) | MIC (MS-942) (mg/mL) | MIC (<i>M. tuberculosis H₃₇ Rv</i>) |
| Peceol | 3–4 | 41.3±1.8 | 17.9±1.1 | 18.8±2.0 | – |
| Captex 355P | < 1 | 17.8±1.0 | 22.7±1.9 | 20.3±1.6 | – |
| Capmul MCM | 5.5 | 56.9±1.8 | 12.5±0.5 | 12.5±0.4 | 18.4±1.5 |
| Capmul PGMC | 5–6 | 84.5±1.7 | 27.3±3.5 | 36.2±2.2 | – |
| Capmul PG8 | 6.7 | 173.8±13.2 | 5.4±0.02 | 5.8±0.01 | 10.2±0.3 |
| Miglyol 812 | < 1 | 12.8±0.6 | 15.7±1.8 | 19.6±2.3 | – |
| Labrasol | 14–16 | 32.9±2.3 | 25.0±1.0 | 25.0±1.0 | 30.8±7.2 |
| Oleyl amine (0.05% w/w) | NA | 10.6±0.5 | 29.5±4.2 | 26.4±3.2 | 38.2±2.7 |
| Tween-80 | 15 | 17.9±1.0 | 18.2±1.0 | 23.2±1.0 | – |
| Transcutol HP | 4.2 | 58.2±2.8 | 00.0±0.0 | 00.0±0.0 | – |
| Cremophor-EL | 12–14 | 17.3±1.0 | 00.0±0.0 | 00.0±0.0 | – |
| Acconon MCB | 14–15 | 35.3±2.1 | 10.6±0.3 | 13.2±0.1 | 15.6±3.2 |
| Propylene glycol | 11.6 | 19.1±1.3 | 19.8±3.1 | 26.1±1.9 | – |

Note: Data are presented as mean ± standard deviation (n = 3).

Abbreviations: NA, not applied; MIC, minimum inhibitory concentration.

which no colonies were observed. All experiments were performed in triplicate.

Susceptibility of *M. tuberculosis* H₃₇Rv was evaluated. Cultures (OD₅₉₅ ~ 0.5) in Middlebrook 7H9 broth (Difco Laboratory, USA) supplemented with albumin dextrose complex were sub-cultured under aerobic conditions at 37 ± 1°C. The sub-cultured strain was streaked using one loopful equivalent to 6.0 µL, with a 3-mm diameter on 25 mL of Lowenstein-Johnsen media (LJ media) in a loosely capped McCartney vial. The culture was then incubated for 12 hrs. After 12 hrs, the cap was tightened and the vial was inverted for 6 weeks at 37 ± 1°C (incubated in inverted position). For the positive control group, no drug was added. Buff-colored colonies were counted after completion of the incubation period, and vials that did not contain colonies were considered to have been treated at the MIC. The study was performed in class II biological safety cabinets.¹⁵

Preparation of RIF-Loaded Nanoemulsion and Phase Diagram Construction

Following the selection of lipid, surfactant, and co-surfactant components, pseudo-ternary phase diagrams (TPD) were established for RIF delivery. To induce a positive charge, oleylamine was added (0.01% w/v) to the organic phase. Capmul PG8 was chosen as the lipid, labrasol was chosen as the surfactant, and acconon MC8 (AC8) was chosen as the co-surfactant. Several trial formulations were produced using a slow and spontaneous emulsification (aqueous phase) titration method.^{16–18} To construct clear and stable oil in water (o/w) nanoemulsions, labrasol (high HLB = 14) is required (HLB > 11) in combination with co-surfactant. Capmul PG8, LAB, and AC8 exhibited maximum solubility, therefore, surfactant was minimized in the final formulation as a safety measure. The LAB:AC8 ratio (S_{mix}) was evaluated at 1:2, 1:3, 3:1, and 2:1 to generate phase diagrams of stable nanoemulsions loaded with RIF at room temperature (Figure 1). The TPDs for these formulations were generated using slow titration to determine the ideal S_{mix} and CPG8 concentration. A series of combinations (Oil:S_{mix}) were evaluated to determine the boundaries of the phase diagram when S_{mix} was 1:2, 2:1, 3:1, or 1:3 (Table 2). Rifampicin (100 mg) was completely solubilized in capmul PG8 containing oleylamine (0.05% w/v) as a cationic charge inducer. Each S_{mix} ratio was added separately to the oil phase then vortexed to obtain a homogenous and clear pre-concentrate. The resulting pre-concentrate was gradually titrated with an aqueous medium to generate a stable

nanoemulsion. This resulted in several formulations, which were observed for bench top stability for 24 hrs. All TPDs were constructed using Pro-origin 6.0 software (Microcal Software Inc., Northampton, MA). The optimized formulation (1 mL) was incorporated into 1% carbopol gel (carbopol 934) to a final concentration of 10% RIF (w/w) in 0.5% gel (w/w).

Characterization of Nanoemulsions

The developed formulations were evaluated for globular size and size distribution using DLS (dynamic light scattering) and a Zetasizer Nano ZS (Malvern Instruments, Worcestershire, UK).¹⁹ This technique is non-destructive and is suitable for the measurement of globular size in the submicron region. Furthermore, size distribution was evaluated and expressed as PDI (polydispersity index). Each formulation was diluted 100× with distilled water to ensure complete dispersion before measurement, and the samples were analyzed at 25°C with a scattering angle of 90°. Gel formulations (100 mg) were dispersed in distilled water (100 mL), and globular size was determined. Zeta potential was determined without dilution using a 4.0 mW He-Ne red laser (633 nm) to measure the surface charge from -120 to 120 mV.²⁰ The pH values of all formulations were determined using an HI 9321 pH meter (an electrode meter) (Hanna Instruments, Ann Arbor, MI, USA).

Morphological assessments (globular size and shape) of the selected nanoemulsions (undiluted) and the subsequent gels (diluted) were investigated using transmission electron microscopy (TEM) (Tecnail 2120 KV, FEI Company, Eindhoven, the Netherlands). A drop of sample was gently placed on a copper grid previously coated with carbon. The sample was negatively stained (2% w/v phosphotungstic solution) prior to analysis. The specimen was then visualized using a transmission electron microscope. The images were scanned at various magnifications, and the estimated globular size using TEM was different than that determined using the Zetasizer instrument.¹⁶ This variation was expressed as “fold-error” estimated using the following Equation (1):

$$\text{Fold-error} = 10^{\text{Log}(\text{particle size, TEM}/\text{particle size, zetasizer})} \quad (1)$$

$$\text{Z-average mean size}(D_z) = [(\sum S_i)/\sum(S_i/D_i)] \quad (2)$$

where D_z represents hydrodynamic diameter (intensity-based harmonic mean) of the globular particle. S_i and D_i indicate the scattered intensity of particle i and the diameter of particle i , respectively.

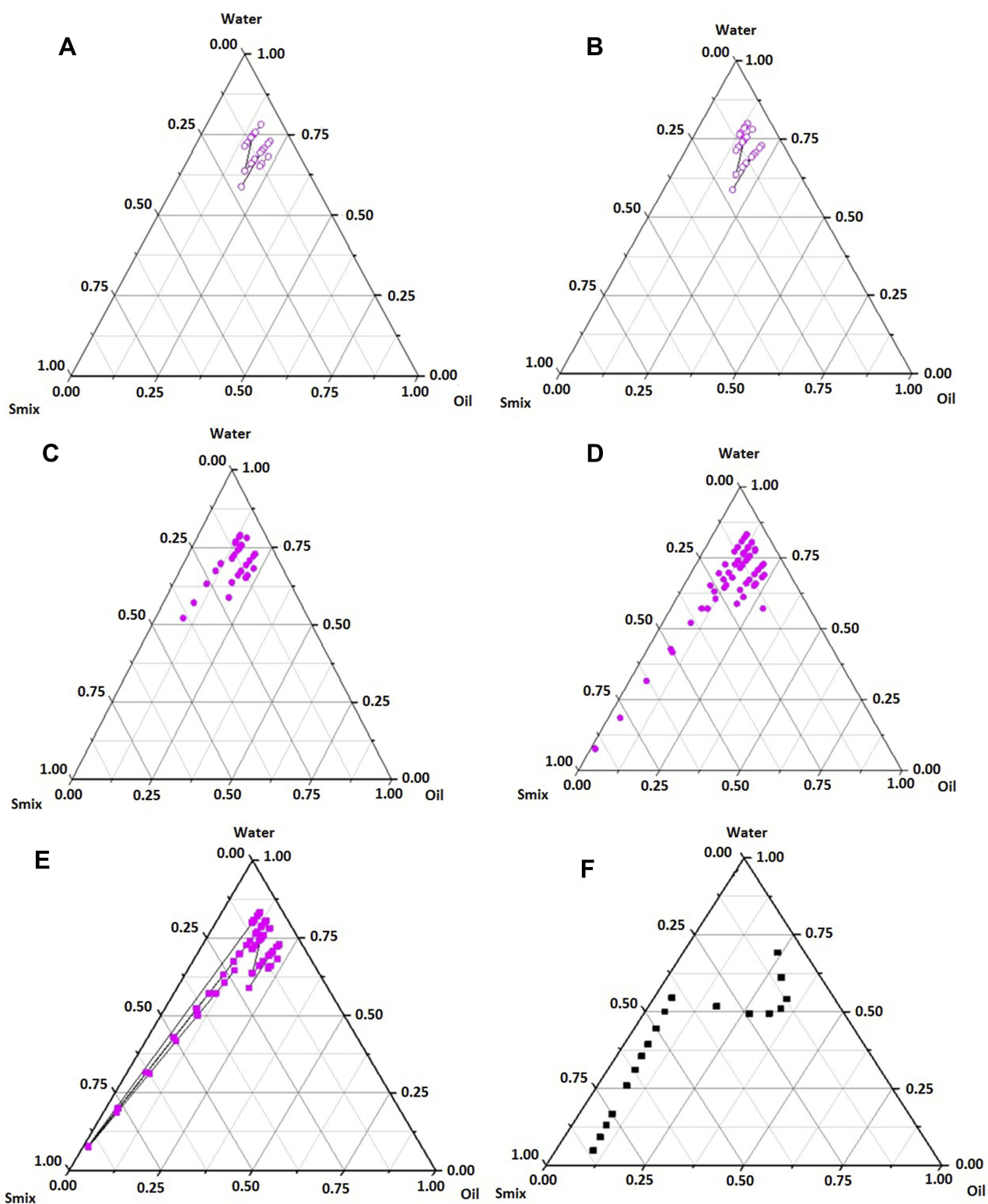


Figure 1 Pseudo-ternary phase diagram for RIF-loaded nanoemulsions.

Notes: (A) CNE-I with S_{mix} ratio 2:1, (B) CNE-II with S_{mix} ratio of 2:1 and 15% oil, (C) CNE-III with S_{mix} ratio of 1:2 and 7.5% oil, (D) CNE-IV with S_{mix} ratio of 3:1 and 15% oil, (E) CNE-V with S_{mix} ratio of 1:3 and 7.5% oil, and (F) CNE-VI with S_{mix} ratio 1:2 and 15% oil.

Rheological Study

The rheological properties (viscosity, cP) of the formulations (nanoemulsions and gel) were determined. Viscosity

(η , an ideal flow characteristic) was measured using a Brookfield viscometer equipped with a coaxial cone and plate (Bohlin Visco 88, Malvern, United Kingdom). This

Table 2 Composition and Evaluation Parameters of Selected Rifampicin (100 Mg) Loaded Cationic Nanoemulsions Containing Constant Amount of Oleylamine (0.05% w/v) as Cationic Charge Inducer

| Formulation Code | Oil (% w/w) | S _{mix} Ratio | Aqueous (% w/w) | Mean Droplet Size (nm) | Polydispersity Index | Zeta Potential (mV) | Viscosity (cP) | pH |
|------------------|-------------|------------------------|-----------------|------------------------|----------------------|---------------------|----------------|-----|
| CNE-I | 7.5 | (12.5) 2:1 | 79.5 | 191.5±13.8 | 0.45 | +15.16 | 30.26 ±1.8 | 7.5 |
| CNE-II | 15 | (30.0) 2:1 | 54.5 | 225.7±11.9 | 0.64 | +12.27 | 26.11±1.4 | 7.9 |
| CNE-III | 7.5 | (12.5) 1:2 | 79.5 | 101.0±6.9 | 0.54 | +22.12 | 40.4±1.2 | 7.7 |
| CNE-IV | 15 | (30.0) 3:1 | 54.5 | 89.8±11.4 | 0.12 | +32.81 | 35.4±1.4 | 7.4 |
| CNE-V | 7.5 | (12.5) 1:3 | 79.5 | 110.5±5.9 | 0.34 | +18.19 | 37.9±1.7 | 7.5 |
| CNE-VI | 15 | (30.0) 1:2 | 54.5 | 145.6±2.1 | 0.48 | +13.37 | 35.3±1.2 | 7.8 |

Note: Data presented as mean ± standard deviation (n = 3). Transcutol-HP as permeation enhancer across the skin. S_{mix}, surfactant: co-surfactant ratio.

study used spindle #S01 at ambient temperature ($25 \pm 1^\circ\text{C}$) and at shear rates between 12.28 and 120.5 s^{-1} . The obtained viscosity values were expressed as a function of the shear rates. The formulations were processed at various spindle rotation speeds (0.5, 1, 2, 3, 4, 5, 10, 20, 30, 50, 60, 70, 80, and 100 rpm) for 50 min.^{19,20}

Full Factorial Design: Experimental Design Tool

Experimental design techniques were used to obtain the most robust formulation within the optimal range of excipients. In this study, a 3^2 (level^{independent variables}) full factorial experimental design (FFD) was used in which two-factors (independent variables) at three-levels (low, high and intermediate) were optimized for responses using Design Expert[®] software (version 8.0.7.1, Stat-Ease, Inc., Minneapolis, MN).¹⁷ In this FFD, the selected factors were S_{mix} (LAB and AC8) and lipid (CPG8), with RIF solubility and MIC values against non-virulent (MS 995 and MS 942) and experimental *Mycobacterium tuberculosis* H₃₇ Rv strains as responses (Table 1). Three levels of the two selected factors (S_{mix} as X₁ and CPG8 as X₂) were evaluated against four dependent responses, including globular size (Y₁, nm), zeta potential (Y₂, mV), drug deposition (Y₃, $\mu\text{g}/\text{cm}^2$), and permeation flux (Y₄, $\mu\text{g}/\text{hr cm}^2$) (Table 3). Levels of S_{mix} (X₁) and CPG8 (X₂) were denoted as (+) for maximum, (0) for intermediate, and (−) for minimum. Optimization consisted of a total of nine experimental runs. Linear equations were generated by the software as $Y = b_0 + b_1X_1 + b_2X_2$, where Y was the measured response, b₀ was the intercept, and b₁ and b₂ were linear coefficients.¹⁷ A statistical analysis was performed to identify major independent factors that affected the responses, and to determine interactions between the factors, which resulted in the selection of the most robust formulation.

Percent Encapsulation Efficiency Study

To determine drug encapsulation efficiency, nanoemulsion formulation samples (1 mL) were added to Eppendorf centrifuge tubes, then subjected to ultracentrifugation (Beckman Optima L-80, Beckman, Brea, CA, USA) at $13,000 \times g$ for 2 hrs to obtain a clear supernatant.²¹ The supernatant solution (0.1 mL) was withdrawn and stored at 4°C until analysis. The supernatant was diluted with a 1:1 (v/v, 2.9 mL) methanol:water mixture to determine RIF content, and %EE was calculated using the following equation (3):

$$EE(\%) = (E_2/E_1) \times 100 \quad (3)$$

where E₁ and E₂ were the total drug content added to the formulation and the total free amount of drug, respectively. Rifampicin content was analyzed using a UV-Vis spectrophotometer at 337 nm.

Hemolysis Measurement

To minimize hemolysis induced by the optimized formulations, hemocompatibility was evaluated by performing an in vitro hemolysis study as previously reported.^{22,23} Each formulation (nanoemulsion and respective gel) was diluted with distilled water to 40 $\mu\text{g}/\text{mL}$ (equivalent to the target flux into the systemic circulation) and 400 $\mu\text{g}/\text{mL}$ (10-fold higher than the target flux value). In this study, OCNE-1 (40 $\mu\text{g}/\text{mL}$), OCNE-1 (400 $\mu\text{g}/\text{mL}$), OCNE-1 Gel (40 $\mu\text{g}/\text{mL}$), OCNE-1 Gel (400 $\mu\text{g}/\text{mL}$), OCNE-1T Gel (40 $\mu\text{g}/\text{mL}$), OCNE-1T Gel (400 $\mu\text{g}/\text{mL}$), OCNE-1 placebo, gel (0.5% w/w), distilled water (positive control), and PBS-7.4 (negative control) were evaluated. Erythrocytes (RBCs) suspended in saline (4%, v/v) were prepared from healthy rats. Each sample (1 mL) and RBC suspension (0.5 mL) were collected in tubes containing Na₂EDTA (disodium ethylenediaminetetraacetic acid). Then, 1.5 mL of PBS

Table 3 Independent Variables (X), Responses (Y) and Statistical Models for Rifampicin-Loaded Cationic Nanoemulsion Formulations in Experimental Design

| Independent Variables | Levels | | | | | |
|--|----------------|----------------|-----------------|----------------|----------------|----------------|
| | Low | | Middle | | High | |
| | Coded | Actual (mg) | Coded | Actual (mg) | Coded | Actual (mg) |
| A=X ₁ : S _{mix} | (-1) | 100.0 | (0) | 300 | (+1) | 500.0 |
| B=X ₂ : Capmul PG8 (CPG8) | (-1) | 75.0 | (0) | 187.5 | (+1) | 300.0 |
| Dependent variable | Constraints | | | | | |
| | Low | | High | Target | | |
| Y ₁ : Particle size (nm) | 89.8 | | 225.8 | Minimum | | |
| Y ₂ : Zeta potential (mV) | +12.3 | | +32.8 | Maximum | | |
| Y ₃ : Drug deposition (%) | 16.1 | | 45.1 | Maximum | | |
| Y ₄ : Skin permeation flux (µg/cm ² /hr) | 13.1 | | 38.8 | Maximum | | |
| Formulation code | X ₁ | X ₂ | Y ₁ | Y ₂ | Y ₃ | Y ₄ |
| CNE1 | (-1) | (-1) | 110.7±6.8 | 21.9±1.1 | 19.3±0.5 | 17.4±0.11 |
| CNE2 | (-1) | (0) | 150.2±11.0 | 29.7±1.0 | 22.4±1.2 | 18.3±1.3 |
| CNE3 | (-1) | (+1) | 164.5±9.5 | 32.4±1.7 | 20.3±1.6 | 26.7±1.5 |
| CNE4 | (0) | (-1) | 89.8±4.1 | 23.1±0.9 | 16.1±0.7 | 30.8±1.8 |
| CNE5 | (0) | (0) | 120.8±7.7 | 27.8±0.7 | 24.8±1.0 | 19.1±0.8 |
| CNE6 | (0) | (+1) | 178.7±10.3 | 31.1±1.8 | 30.2±1.3 | 25.3±1.0 |
| CNE7 | (+1) | (-1) | 190.6±12.5 | 12.3±0.2 | 35.2±0.9 | 24.8±1.5 |
| CNE8 | (+1) | (0) | 105.3±16.4 | 22.1±0.9 | 38.7±0.8 | 39.3±0.5 |
| CNE9 | (+1) | (+1) | 225.7±13.9 | 32.8±1.8 | 45.1±1.5 | 34.8±1.0 |
| Composition of final optimized OCNE-1 | | | Y ₁ | Y ₂ | Y ₃ | Y ₄ |
| Smix: 459.5 mg (3:1) CPG8: 187.5 mg Desirability: 0.989 | | | 97.25 (101.14)* | 22.21 (23.81)* | 14.34 (16.37)* | 34.67 (36.96)* |

Note: *Data presented as predicted values (observed values).

was added to a final volume of 3 mL. All samples were incubated at 37 ± 1 °C for 2 hrs without agitation. After incubation of the test sample with RBCs for 2 hrs, the samples were centrifuged at 3000 rpm for 15 min to obtain a pellet of RBC debris and serum protein. Hemoglobin (Hb) released following interaction with erythrocytes or lysed RBCs was analyzed in the supernatants (0.5 mL of supernatant diluted with 2.5 mL of distilled water) at a λ_{\max} of 540 nm. Total Hb release was estimated using a UV/Vis spectrophotometer and expressed as a percentage. The positive control was considered to cause 100% lysis. Percent hemolysis was calculated using the following equation (4):

$$\% \text{ Hemolysis} = [(A_S - A_N) / (A_P - A_N)] \times 100 \quad (4)$$

where A_S represented the absorbance value of the test sample, and A_N and A_P were the absorbance values of the negative and positive controls, respectively.

Spreadability Assessment

Spreadability of transdermal delivery systems is an important measure of ease of application, and was evaluated as previously described.²⁴ Each gel formulation (OCNE-1 gel placebo, OCNE-1 gel, and OCNE-1T gel; 1.0 ± 0.02 g each) was cast into a cylindrical shape with a fixed surface area (0.88 cm^2) using a microtome. The formulations were then pressed with various weights (50, 100, 200, and 500 g for 1 min each) between the flat surface of a graduated glass plate (6×6 , 25 g) and the microtome at room temperature (25 °C). Total area and change in area (cm^2) were determined as a function of weight applied (g). Gels that leave a thin film after topical application are stable and demonstrate thixotropic behavior.²⁴ The percent spread was calculated using the following equation (5):

$$\% \text{ Spread by weight} = [(W_1 - W_2) / W_1] \times 100 \quad (5)$$

where W_1 and W_2 represented the initial and final weights, respectively.

Drug Release Study

In vitro drug release of RIF from OCNE-1, DS (RIF injection), OCNE-1 gel, and OCNE-1T gel was evaluated over a 12 hrs period using a dialysis membrane (Himedia, Ltd., Mumbai India, molecular weight cut-off 12,000–14,000 Dal). To maintain sink conditions in the release medium (200 mL of PBS at pH 5.5), dimethyl sulfoxide (5% w/v) was added to facilitate diffusion and dissolution. Dialysis membrane bags containing formulations with ~100 mg of RIF were placed into the receptor compartments of glass beakers (250 mL). Drug was released into medium maintained at $32 \pm 1^\circ\text{C}$ with constant stirring at 100 rpm for 12 hrs.²⁵ One milliliter of sample was removed at 0.5, 1, 2, 4, 6, 8, 10, and 12 hrs, with replacement. The samples were filtered, and drug content was analyzed using a validated UV/Vis spectrophotometric method. Zero order, first order, and Higuchi models were used to fit the in vitro drug release patterns and determine the mechanisms of release.

Ex vivo Skin Permeation and Drug Deposition Studies

Formulations intended for transdermal delivery require skin permeation studies to determine the skin permeation coefficient (P_c), cumulative amount of drug permeated, lag time, permeation flux (targeted flux), and enhancement ratio to demonstrate efficacy. All animal studies were approved by the Institutional Animal Ethics Committee (IAEC), Department of Pharmaceutical Sciences and Technology, Birla Institute of Technology, Mesra, Ranchi, Jharkhand India.¹⁷ This study was conducted in accordance with the “Organisation for Economic Co-operation and Development” guidelines 402 and 410 (OECD Guidelines, 1981, 1987). All rats (Sprague Dawley) were housed (air conditioned) under appropriate hygienic conditions with sufficient food and water. The rats were fasted for 12 hrs prior to use in experiments. The animals were then sacrificed by cervical dislocation, and the abdominal skin was excised for further skin processing, which included removal of hair, adhered fatty debris, underlying fat, and subcutaneous tissue. All in vivo experiments were performed in compliance with the guide for the care and use of laboratory animals (NC3Rs, ARRIVE guidelines).

The investigation was carried out using Franz diffusion cell in which 3.104 cm^2 and 22.5 mL were exposed diffusion

area and receptor volume, respectively.²⁶ The skin was placed between the donor and receptor chambers such that the dermis side touched the receptor medium (PBS, pH 7.4). The receptor chamber was constantly stirred using an inert magnetic bead (100 rpm) at $32 \pm 1^\circ\text{C}$ (skin temperature). One milliliter was sampled at each time point with replacement at 0.5, 1, 2, 4, 6, 8, 10, 12, 16, 20, and 24 hrs. The withdrawn samples were filtered using membrane filters prior to analysis at 337 nm using a validated UPLC method. Drug solution (0.1 mg/mL) was used as a control. To evaluate drug penetration into rat skin, the formulation remaining on the skin surface was removed by gentle washing with PBS (pH 7.4) at the end of the experiment (24 hr). The mobile phase was acetonitrile (ACN) with methanol (70:30) and 2 mM ammonium acetate buffer (80:20 v/v), and was filtered through a $0.45\text{-}\mu\text{m}$ membrane filter and degassed. The flow rate was 0.5 mL/min, the run time was 3.5 min, and the injection volume was 5 μL . A linear calibration curve for RIF was prepared in rat plasma, and the coefficient of determination (r^2) was 0.99. The calibration curve was linear from 12.27 to 7999.92 ng/mL. The lower limit of quantification for RIF was 0.0012 $\mu\text{g/mL}$.

Steady state permeation flux (J_{ss}) was determined from the linear slope of the cumulative RIF permeation curve over a 24 hrs period. The time required to reach the J_{ss} was the lag time (T_L), and the P_c was calculated from the flux and the initial amount (C) of RIF loaded onto the skin ($P_c = J_{ss}/C$). The targeted flux was calculated using the following equation (6) to ensure the therapeutic effectiveness of the developed formulation.²⁷

$$\text{Targeted flux} = (C_{ss} \times C_t \times \text{BW})/A \quad (6)$$

where C_{ss} = steady state concentration of RIF in human plasma (8–29 $\mu\text{g/mL}$) as the therapeutic window, C_t = total body clearance (3.5 mL/min/kg, 0.058 mL/hr/kg), BW = standard body weight of a human subject (60 kg), and A = area of application on the skin (2.34 cm^2).

The calculated target flux range for RIF was 10.25–37.17 $\mu\text{g/cm}^2\text{ hr}$. This provided a rough estimate of the amount of RIF expected to flux to the plasma through transdermal delivery. However, in vivo pharmacokinetic studies were performed because dermal diffusion rates are dynamic in vivo, but are static in vitro.²⁸

Drug retention in the skin was evaluated. After completion of the ex vivo skin permeation study, the area of skin to which RIF was applied was excised, washed, and sliced into small pieces using surgical scissors. The pieces were placed in a beaker containing 10 mL of 1:1 (v/v)

methanol:chloroform (1:1) then stirred for 10 hrs to extract RIF. The extract was filtered through a 0.22- μ m membrane filter, centrifuged, and the supernatant was analyzed to determine RIF content.

Ex vivo Globule–Skin Interaction Study

To investigate globule interaction with the skin, and perturbations caused by topical application of the formulations, scanning electron microscopy (SEM) was used to visualize the skin.²⁹ Rats were placed in groups. Group I was the control (untreated), and group-II, group-III, and group-IV received OCNE-1, OCNE-1 gel, and OCNE-1T gel, respectively. Each 100 mg formulation contains 10 mg RIF (100 mg/g). After completion of the ex vivo study, the adhered sample on the epidermis was removed carefully, and the skin specimen was sliced using a microtome. The slices were fixed in 10% glutaraldehyde overnight.³⁰ The specimens were then air dried on glass coverslips and coated with gold for SEM (Carl Zeiss, EVO43, SEM, Germany).

In vivo Studies

Pharmacokinetic Evaluation. A pharmacokinetic study was performed using Sprague Dawley (SD) rats ($n = 6$; 200–300 g, and 6–8 weeks old). All animals were housed with free access to water and food at $25 \pm 1^\circ\text{C}$ with 45–55% relative humidity and a 12 hrs light/dark cycle. The animals were cared for in accordance with OECD guidelines 402 and 410 (OECD Guidelines, 1981, 1987).²³ Prior to commencement of the study, the animals were randomly distributed into two groups (A and B), with $n=6$ in each group. Group A received oral RIF suspension (2% sodium carboxymethylcellulose; 10.0 mg of RIF), and group B received transdermal OCNE-1T gel (100 mg of formulation containing 10 mg RIF). The dorsal application site (1 cm^2) was shaved carefully, and the application site was protected using a soft net to avoid removal of the applied gel.

After dosing, blood samples were collected in tubes containing Na_2EDTA from the retroorbital sinuses. The blood samples were centrifuged at $2240 \times g$ for 10 min to separate plasma from erythrocytes, and the plasma was stored at -80°C until use. Samples were collected at predetermined time points (1, 2, 4, 6, 8, 12, and 24 hrs) for RIF analysis using a validated UPLC method. Pharmacokinetic parameters were evaluated, including C_{max} (maximum drug content reached to the plasma), T_{max} (time required to achieve C_{max}), $\text{AUC}_{(0 \rightarrow 24)}$ (area under curve, 24 hrs), $\text{AUC}_{(0 \rightarrow \infty)}$ (AUC from 0 to infinity), K_e (elimination rate

constant), $t_{1/2}$, MRT (mean residence time), and $\text{AUMC}_{(0 \rightarrow \infty)}$ (area under first moment curve). These values were determined using GastroPlusTM software version 9.0 (Simulation Plus Inc., Lancaster, USA) in non-compartmental mode. Bioavailability was calculated using the following equations (7–8):

$$\text{Relative bioavailability} = [(\text{AUC})_{\text{oral}}/(\text{AUC})_{\text{iv}}] \times 100 \quad (7)$$

$$\text{Relative bioavailability} = [(\text{AUC})_{\text{Trans}}/(\text{AUC})_{\text{iv}}] \times 100 \quad (8)$$

where $(\text{AUC})_{\text{oral}}$ and $(\text{AUC})_{\text{Trans}}$ were area under the curve obtained following oral delivery of RIF-suspension and transdermal delivery of OCNE-1T gel, respectively, as compared to intravenous delivery.

In vivo Skin Irritancy Study. The cationic nanoemulsion (OCNE-1) and its gels (OCNE-1 placebo, OCNE-1T gel placebo, and OCNE-1T gel) were evaluated for their ability to cause skin irritation. The rats were housed in a controlled environment (25°C and 65% relative humidity) and provided food and water ad libitum. The hair was carefully shaved from the dorsal portion (2.5 cm^2) of the skin using an electric hair trimmer 24 hrs before the commencement of the study.³¹ The rats were placed in five groups ($n=3$ each). Groups I and II received placebo OCNE-1 nanoemulsion and OCNE-1T gel placebo, respectively. Groups III and IV were treated with OCNE-1 nanoemulsion and OCNE-1T gel, respectively. Group V was treated with 5% sodium lauryl sulfate as a positive control. Formulations (100 mg) were applied at the marked area, and the area was inspected visually for any changes in texture, lesions, redness, irritation, or other abnormalities. Changes were scored according to Draize's scale.³² The application area was scored based on visual dermal reactions (erythema and edema) at predetermined time points (0, 24, 48, and 72 hrs). These scores were expressed as mean values of erythema or edema based on severity: absence of erythema/edema = 0, slight erythema/edema = 1, moderate erythema/edema = 2 and severe erythema/edema = 3.²³

Results and Discussion

Screening of Excipients

Rifampicin was successfully solubilized in lipids and surfactants for the development of nanoemulsions. Rifampicin was soluble in CPG8 (173.8 ± 13.2 mg/mL), LAB (32.9 ± 2.3 mg/mL), and AC8 (35.3 ± 2.1 mg/mL)

(Table 1). Rifampicin was soluble in Transcutol-HP at 58.2 ± 2.8 mg/mL. Higher rifampicin solubility in Transcutol may have been due to lower hydrophilic–lipophilic balance than that of LAB or AC8 (Table 1).^{14–16} Labrasol, CPG8, and AC8 had MIC range values of ~ 25 mg/mL, ~ 5 – 6 mg/mL, and ~ 10 – 14 mg/mL, respectively, against the both non-pathogenic strains (MS-995 and MS-942), and 30.8 ± 7.2 mg/mL, 10.2 ± 0.3 mg/mL, and 15.6 ± 3.2 mg/mL, respectively, against the pathogenic strain. *Mycobacterium smegmatis* was used because it grows rapidly, has been widely used for molecular analysis, is a suitable alternative model to study the pathogenesis of virulent strains (*tubercle bacilli*) under normal laboratory conditions, is unable to enter epithelial cells or phagocytic cells, and has a short generation time (3–4 hrs).^{33,34} Capric and caprylic acid contents ($\sim 80\%$) of the excipients evaluated in this study (LAB and CPG8) were a primary factor in the evaluation of efficacy against *Mycobacterium* strains.¹⁵ Previous studies showed that medium-chain fatty acids and free fatty acids exhibited antimicrobial activity against an array of microorganisms, and a recent study showed that a nanoemulsion comprised of glyceryl monocaprylate and LAB exerted antibacterial effects against *E. coli* and *S. aureus*.^{35–38} These results indicated that LAB, CPG8, and AC8 were suitable as excipients for the development of nanoemulsions.

Preparation of Nanoemulsions

Capmul PG8, LAB, and AC8 were finally selected as the oil phase, surfactant, and co-surfactant, respectively, for the construction of TPDs. Several formulations were prepared with different S_{mix} ratios, and six formulations were stable and did not exhibit phase separation or turbidity (Figure 1A–F). A constant amount of oleylamine (0.05% w/v) was added as a cationic charge inducer to help stabilize the formulations and to allow for efficacy against negatively charged bacilli.³⁷ The cationic nanoemulsion with S_{mix} ratio of 3:1 had a globular size of 89.8 ± 11.4 nm, PDI of 0.12, zeta potential of $+32.81$ mV, and viscosity of 35.4 ± 1.4 cP, which were the best values among the formulations for delivery across the skin. The formulation CNE-IV (S_{mix} ratio of 3:1) exhibited maximum delineated area on the water and S_{mix} axis of the phase diagram as shown in Figure 1D. Reduced globule size may have been due to a high HLB value and LAB concentration compared to a low HLB co-surfactant (Transcutol).³⁶ Each milliliter of formulation contained 100 mg of RIF for topical application. The final pH of CNE-IV was 7.4, which was compatible with bodily fluids. Reduced acid degradation and increased

solubility and permeability of RIF have been reported at pH 6.8 due to the amphoteric nature of the drug (isoelectric point ~ 4.8).³⁹ There is no pharmaceutical product currently on the market for transdermal delivery of RIF for therapeutic or prophylactic use against *Mycobacterium* infection. Recently, cationic nanoemulsions have been developed to facilitate cellular internalization due to electrostatic interaction between opposite charges of cells and globules, promote efficient cytoplasmic delivery and low cytotoxicity, improve colloidal stability when used in conjunction with non-ionic surfactants, confer thermal stability during autoclaving without no change in particles size, and reduce aggregation (Oswald ripening) due to repulsion.⁴⁰ Singh et al showed that cationic nanoemulsions with optimized proportions of oil, surfactant, and oleylamine exhibited innate antibacterial activity against gram-positive and gram-negative strains.^{36–38} This study demonstrated that doses could be reduced due to synergistic antibacterial effects of LAB, CPG8, AC8, and RIF, and reduced side effects. Moreover, topical application of a RIF-loaded nanocarrier could clear *Mycobacterium* residing in the skin and macrophages.

Characterization of CNE-I to CNE-VI Formulations

Six stable formulations (CNE-I to CNE-VI) with different S_{mix} ratios were characterized for globular size, size distribution (polydispersity index), zeta potential, viscosity, and pH (Table 2). Particle size and PDI ranged from 89.8–225 nm and 0.12–0.64, respectively. Figure 2A–D summarizes the development of CNE-IV and shows particle size, pure crystalline RIF, the CNE-IV product, and TEM images. The formulation CNE-IV, with S_{mix} ratio of 3:1, had a small particle size, which was optimal for transdermal permeation of RIF due to the relatively higher concentration of LAB (surfactant) compared with AC8 (co-surfactant) (Figure 2A). Formulations CNE-I (191.5 nm) and CNE-II (225.7 nm) had the same S_{mix} ratio (2:1), but differed in globule size because of higher oil content in CNE-II. Thus, relative increases in oil content compared to S_{mix} resulted in poorer emulsification and increased globule size. We reported a similar trend in which a progressive increase in globular size (from 14.15 nm to 298.1 nm) was observed with increased capmul MCM C8 concentration with constant LAB concentration.¹⁷ Each of the six formulations had positive zeta potentials ranging from $+12.27$ to $+32.81$ mV due to the charge inducer included in the oil phase. The zeta potential was sufficient to stabilize the nanocarriers upon

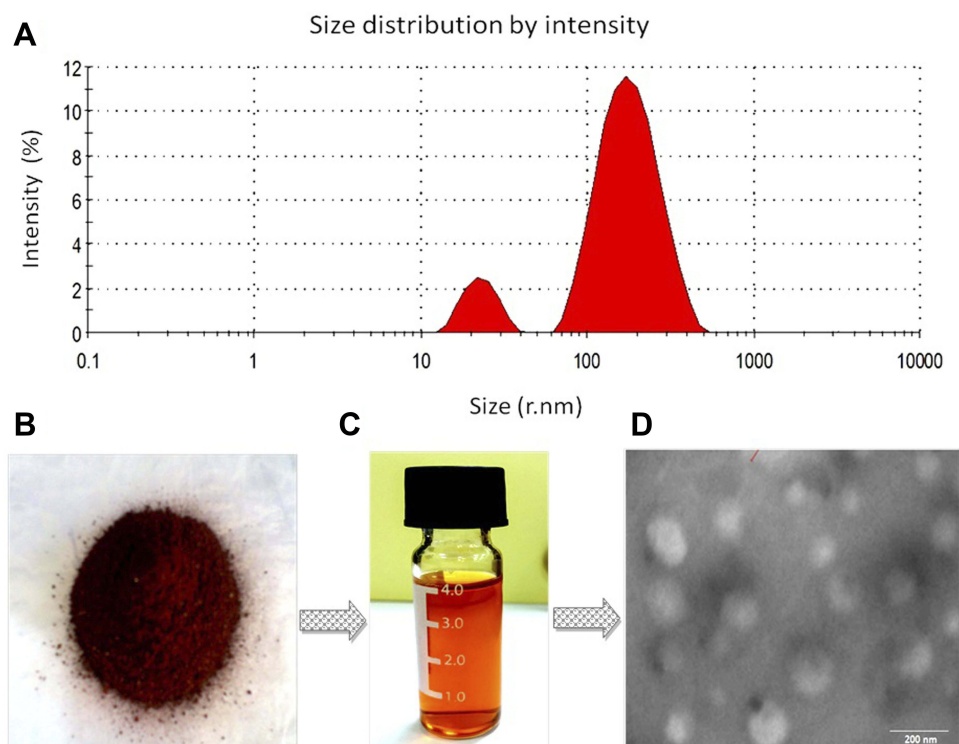


Figure 2 Characterization of the optimized formulation OCNE-I.

Notes: (A) Globular size and intensity, (B) crystalline rifampicin powder, (C) transformed rifampicin-loaded nanoemulsion, and (D) morphological assessment of OCNE-I nanoemulsion using transmission electron microscopy, which showed spherical, non-aggregated particles (scale 200 nm).

dispersal in the aqueous phase through surface charge density and potential.^{36,37} Viscosity was optimal for each formulation for thin film formation following topical application. The final pH was adjusted to ~7.4 for physiological compatibility. Finally, CNE-IV was the optimal formulation with regard to globular size, spherical shape (Figure 2D), PDI, charge stability, viscosity, and pH (Figure 2). Therefore, CNE-IV was selected for further optimization using Design Expert[®].

Optimization of the Nanoemulsion

The S_{mix} ratio of CNE-IV was kept constant at 3:1 for further optimization of the nanoemulsion using a full factorial experimental design. This program allowed for the selection of independent factors that affected responses while accounting for non-significant factors.¹⁷ This process resulted in the optimization of oil and S_{mix} content. The suggested formulations CNE-1 to CNE-9 are intended for transdermal delivery and were optimized for responses that affect drug diffusion across the skin such as globular size (nm, Figure 3A), zeta potential (mV, Figure 3B), drug deposition (Figure 3C), and permeation flux (Figure 3D).

The globular sizes for the nine optimization formulations (Table 3) ranged from 89.8 to 225.7 nm. Positive signs and the negative signs in the modeling equations signify synergistic and antagonistic effects of each factor against the response, respectively.²⁰ The polynomial mathematical model for the response Y_1 ($Y_1 = 159.6 + 32.75X_1 + 29.6X_2$) showed that increased CPG8 resulted in a significant increase in globular size ($p < 0.026$), which suggested that optimization of CPG8 was critical (Figure 3A). The response Y_2 ($Y_2 = 25.9 - 2.8X_1 + 6.8X_2$) showed that increased S_{mix} resulted in decreased positive surface charge ($p < 0.004$; Figure 3B; Table 4). This might be correlated with the observed finding wherein S_{mix} ratio was found to be inversely proportional to particle size due to facilitated emulsification by the surfactant and the co-surfactant. The observed and predicted values for Y_1 ($r^2 = 0.972$; Table 4) and Y_2 ($r^2 = 0.991$; Table 4; Figure 4A and B) correlated well. Furthermore, there was no interaction between the independent variables X_1 and X_2 and responses Y_1 and Y_2 , respectively.

To obtain a stable formulation, S_{mix} must be at the optimal ratio. The responses Y_3 (drug deposition; $Y_3 = 28.11 + 9.5X_1 + 4.16X_2$) and Y_4 (permeation flux; $Y_4 = 23.72 + 5.08X_1 + 5.8X_2$) were critical to maximizing permeation across the

skin. The results showed that both investigated factors (X_1 and X_2) should be maximized for optimal therapeutic efficacy against *Mycobacterium*. Analysis of Y_3 showed drug deposition ranging from 16.1 to 45.1 $\mu\text{g}/\text{cm}^2$ (Figure 3C), and maximum drug deposition was observed for CNE-9, which may have been due to large globular size. Permeation flux ranged from 18.3 to 39.3 $\mu\text{g}/\text{hr cm}^2$ (Figure 3D). Thus, the responses Y_3 and Y_4 increased with increased X_1 and X_2 content. Solubilization of rifampicin in oil matrix promoted enhanced

drug deposition in the skin, whereas S_{mix} may contribute to temporary perturbation of the SC layer, resulting in enhanced permeation and improved permeation flux. Generally, higher drug deposition results in higher permeation flux. Drug precipitation from the o/w nanoemulsion in the skin strata was not of concern because RIF is lipophilic.⁴¹ In contrast, isoniazid, which is hydrophilic, has been used for sustained topical delivery, which may result from precipitation in lipophilic skin regions.⁴¹

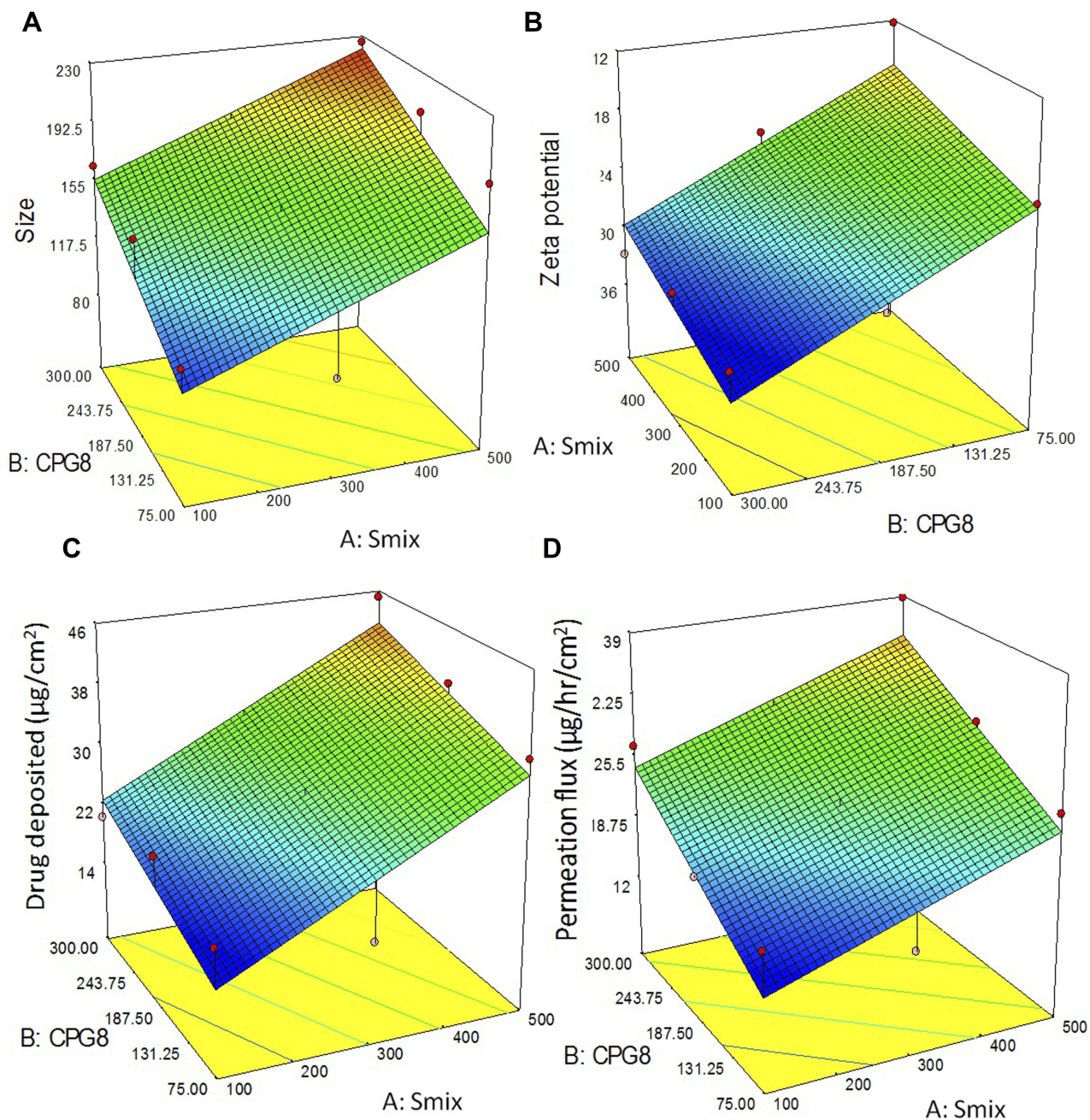


Figure 3 Contour plots of the effects of independent variables on responses.

Notes: (A) Particle size (Y_1), (B) zeta potential (Y_2), (C) drug deposition (Y_3), and (D) permeation flux (Y_4).

The desirability function was used to validate the optimization parameters and to specify constraints for responses. These constraints were “minimize,” “maximize,” “maximize,” and “maximize” for responses Y_1 , Y_2 , Y_3 , and Y_4 , respectively. Because this nanoemulsion was designed for the transdermal application, the goal was to achieve maximal drug deposition in the skin and permeation flux across the skin using a cationic nanocarrier. Maximization of cationic charge improved stability and enhanced cellular internalization due to electrostatic interactions between the nanoemulsion and anionic bacilli cells.^{36,37} Maximization of this parameter did not compromise the maximization of Y_2 , Y_3 , and Y_4 . The overall desirability was maximal (0.989) at a high level of X_1 and an intermediate level of X_2 , as shown in Table 3. A summary of the model for all responses is shown in Table 4. The optimized formulation OCNE-1 was comprised of 59.5 mg of S_{mix} (X_1) and 187.5 mg of CPG8 (X_2). The predicted and observed values for Y_1 , Y_2 , Y_3 , and Y_4 for OCNE-1 are summarized in Table 3.

The influence of the independent variables (X_1 and X_2) on the responses (Y_1 , Y_2 , Y_3 , and Y_4), and the relationships between predicted and observed values is summarized in Figure 3C and D. The results showed a linear increase in drug deposition ($p < 0.005$) and permeation flux with increased CPG8 concentration due to higher drug loading in the oil phase and enhanced permeation enhancement resulting from increased S_{mix} ($p < 0.01$). Good

correlation was observed between the observed and predicted values for Y_3 ($r^2 = 0.981$; Table 4) and Y_4 ($r^2 = 0.984$; Table 4) (Figure 4C and D). There was no interaction between the independent variables X_1 and X_2 for the responses Y_3 and Y_4 , respectively (Figure 5C and D).

Post-Optimization Characterizations

Percent Encapsulation Efficiency (%EE) Study

The encapsulation efficiencies of the developed cationic nanoemulsions are summarized in Figure 6A. The values ranged from 37.0% to 89.7%, and CNE-8 and CNE-4 had % EE values of $89.7 \pm 4.45\%$ and $37.0 \pm 1.85\%$, respectively. Percent EE increased with increased oil content because RIF is lipophilic, as evidenced by high solubility of RIF in CNE-4 and CNE-6. In contrast, a further increase in oil content in CNE-7 resulted in a significant ($p < 0.05$) reduction in %EE, which may have been due to insufficient S_{mix} to allow for emulsification. The results showed that CNE-8 had the highest %EE, and S_{mix} concentration was directly proportional to %EE (Figure 6A).

Hemolysis Assessment

All formulations contained the positively charged component oleylamine as a charge inducer. Therefore, hemolysis was evaluated. The rough estimate of steady state concentration of RIF was approximately 10–40 $\mu\text{g/mL}$. Therefore, formulations (minimum concentration and 10-fold higher concentration) were incubated at room temperature with

Table 4 Model Summary Statistics of Responses with Best Fit Model Equations

| Regression Equations with Best Fitted Model | | | | |
|--|-------------------------------|--------------------------------|-------------------------------|---|
| $Y_1 = 159.6 + 32.75X_1 + 29.6X_2$ $Y_2 = 25.9 - 2.8X_1 + 6.8X_2$ $Y_3 = 28.11 + 9.5X_1 + 4.16X_2$ $Y_4 = 23.72 + 5.08X_1 + 5.8X_2$ | | | | |
| Statistical parameters | Particle size in nm (Y_1) | Zeta potential in mV (Y_2) | Drug deposited in % (Y_3) | Permeation flux ($\mu\text{g}/\text{cm}^2/\text{hr}$) (Y_4) |
| r^2 | 0.972 | 0.991 | 0.981 | 0.984 |
| Adjusted r^2 | 0.96 | 0.93 | 0.97 | 0.96 |
| Predicted r^2 | 0.93 | 0.85 | 0.89 | 0.88 |
| Model f value | 7.03 | 15.63 | 14.23 | 10.36 |
| p value | 0.026 | 0.004 | 0.005 | 0.01 |
| Model | Linear | Linear | Linear | Linear |
| SD | 28.84 | 3.09 | 4.76 | 2.24 |
| Mean value | 159.62 | 25.91 | 28.1 | 23.72 |
| % CV | 18.07 | 11.96 | 17.00 | 17.48 |

Note: Value of regression coefficient represented as r^2 .

Abbreviations: SD, standard deviation; CV, coefficient of variation.

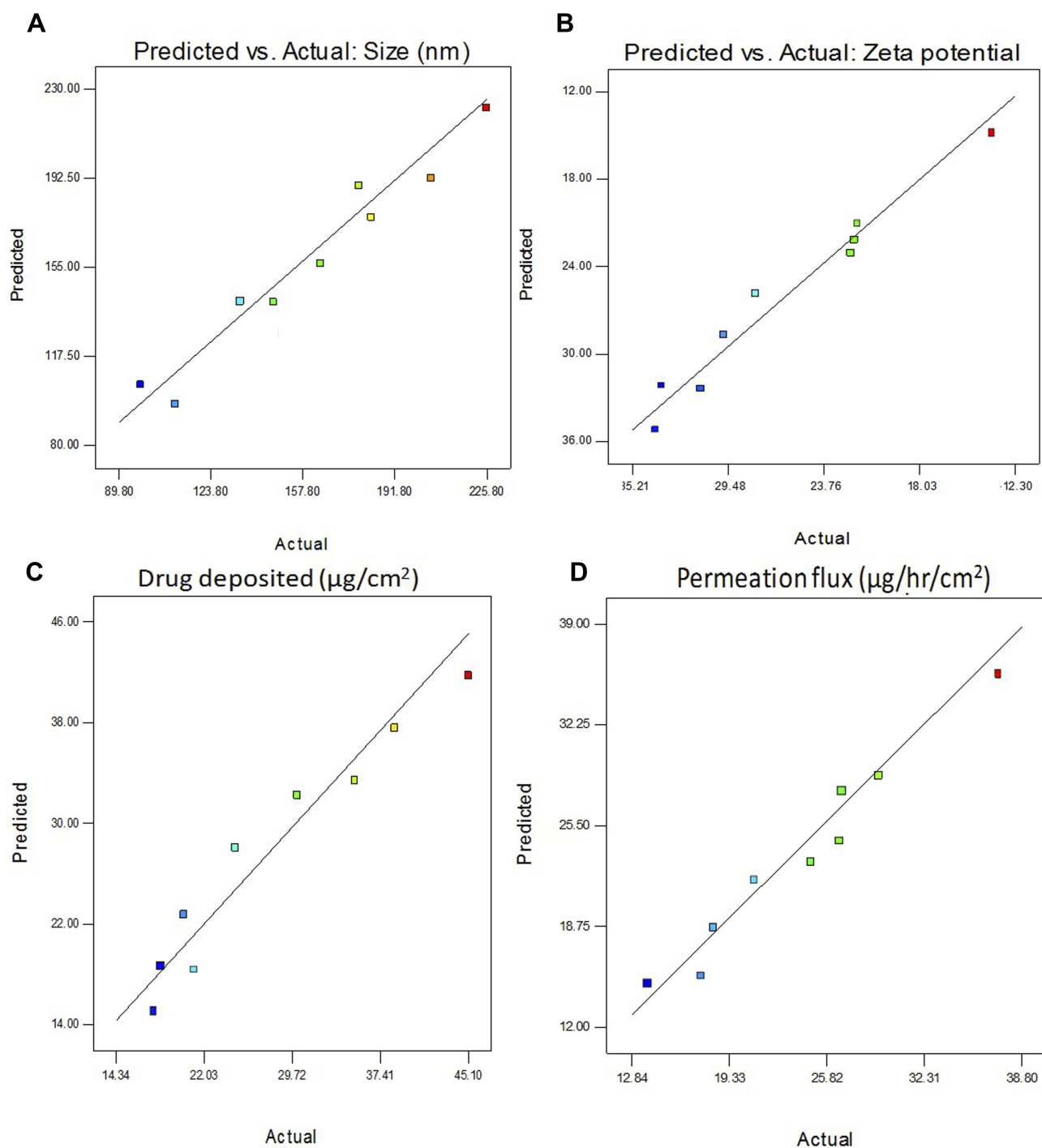


Figure 4 Correlation graph of predicted versus actual values.

Notes: (A) Particle size (Y_1), (B) zeta potential (Y_2), (C) drug deposition (Y_3), and (D) permeation flux (Y_4).

erythrocytes for 2 hrs (Figure 6B). The results showed that all of the nanoemulsions were hemocompatible (hemolysis < 14%) except for the positive control, distilled water (hemolysis = 100%) (Figure 6B). These results agreed

with those from our previous study that evaluated lipid- and surfactant-based nanocarriers for oral delivery,¹⁷ which also showed that cationic nanoemulsions were hemocompatible.

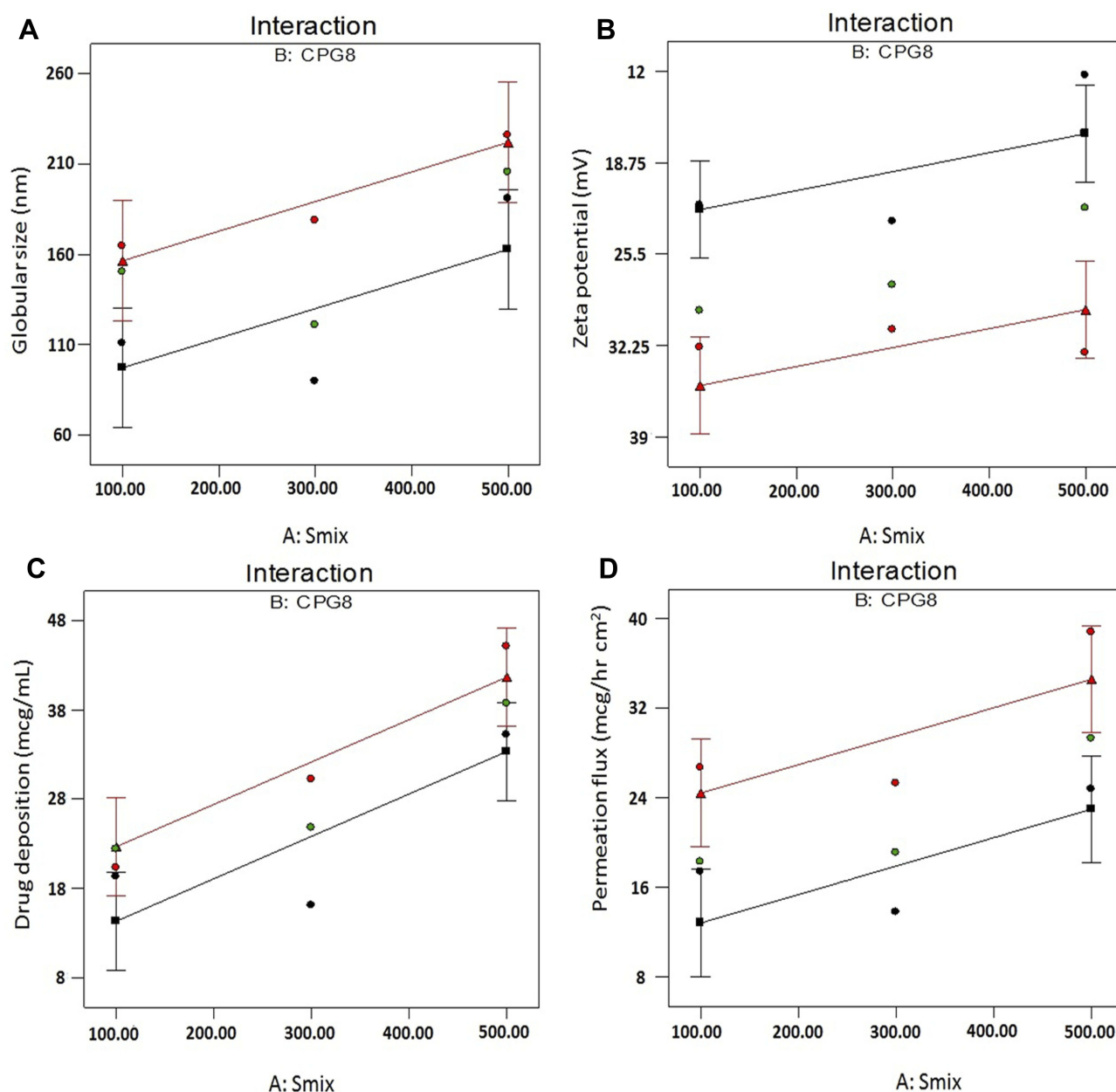


Figure 5 Interaction graph of independent variables.

Notes: (A) Particle size (Y_1), (B) zeta potential (Y_2), (C) drug deposition (Y_3), and (D) permeation flux (Y_4).

Spreadability Study

Spreadability is a measure of ease of application and the extent of thin-film formation following the application of a transdermal formulation on the skin.⁴² Percent spread by weight of OCNE-1 nanoemulsion, OCNE-1T gel, and OCNE-1T gel placebo was $53.09 \pm 1.8\%$, $174.11 \pm 1.8\%$, and $177.57 \pm 3.8\%$. These results showed that the gel formulations had a higher percent spread than the OCNE-1 nanoemulsion, which may have been due to higher viscosity of the gel formulations. There was not a significant ($p > 0.05$) difference in percent spread

between the placebo gel and the RIF-loaded gel. These results showed that the gel formulation was a suitable carrier for extended contact time and enhanced permeation. These results agreed with those observed for a previous gel formulation developed for topical treatment of fungal infections.¹⁴

In vitro Drug Release Assessment

Three optimized formulations (OCNE-1, OCNE-1 gel, and OCNE-1T gel) were compared with DS for RIF release in buffer media (pH 7.4). Drug solution was used as the

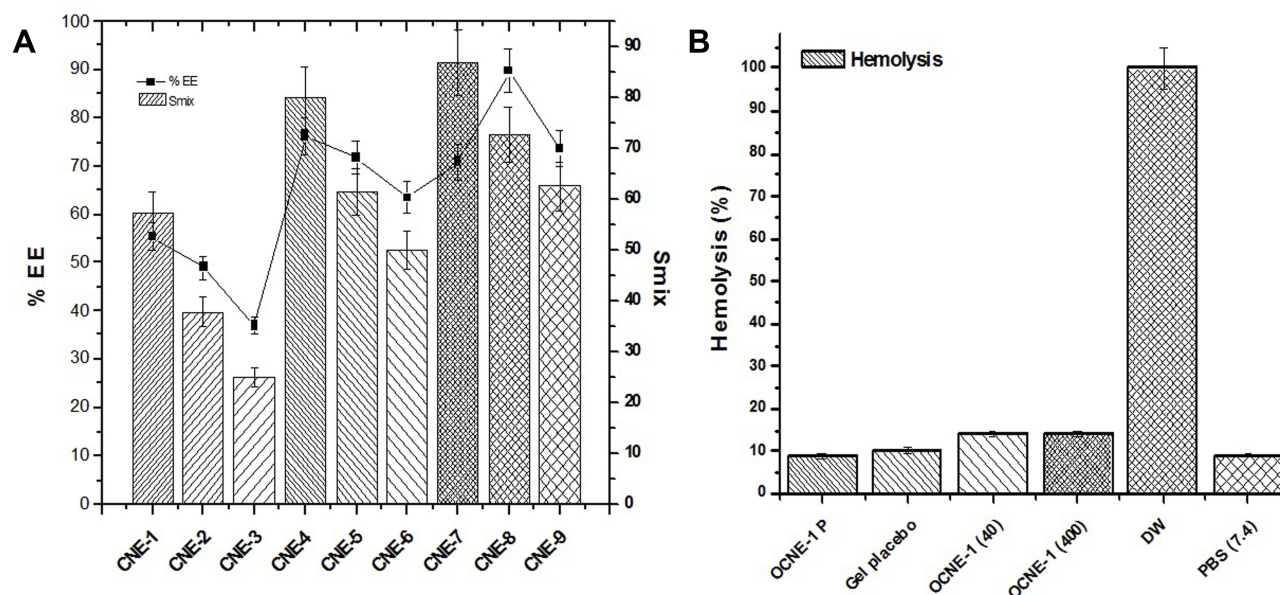


Figure 6 Percent encapsulation efficiency (%EE) and hemolysis studies.

Notes: (A) Effect of S_{mix} concentration on %EE and (B) hemolysis of optimized formulations compared to those of controls (positive and negative control group).

control to ensure that the membrane did not interact with the drug under experimental conditions. The DS showed >94.5% release within 2 hrs, which showed that RIF did not interact with the dialysis membrane. Both gel formulations (OCNE-1 gel and OCNE-1T gel) released more slowly, which may have been due to higher viscosity values (89.21 cP for OCNE-1 gel and 91.548 cP for OCNE-1T gel). The OCNE-1 nanoemulsion exhibited faster drug release due to lower viscosity and transport of RIF in o/w nanoemulsion globules to the membrane, which resulted in the release into the media. Faster release of RIF from OCNE-1 may have also been due to larger surface area resulting from low viscosity. For the gel formulations, the viscous matrix mitigated diffusion of the nanocarriers across the membrane, which resulted in slow and sustained release of RIF. Moreover, the gel carrier improved the residence time of the formulation at the applied site, which suggested that these formulations would augment permeation in an appropriate model. Drug release from OCNE-1 ($57.54 \pm 2.9\%$) was significantly ($p < 0.005$) higher than that from OCNE-1 gel ($19.04 \pm 1.5\%$) and OCNE-1T gel ($32.97 \pm 1.7\%$) within 4 hrs. The OCNE-1T gel contained Transcutol as a permeation enhancer, which may have promoted drug release due to improved solubilization (58.2 ± 0.8 mg/mL) and a lower HLB value (4.3), as shown in Table 1. Release profiles for each formulation over 12 hrs are shown in Figure 7. Release of RIF from OCNE-1 (18.2%) was 5.22-fold

higher than that from DS (94.5%), which indicated slow and sustained drug release across the membrane within the initial 2 hrs. The OCNE-1 nanoemulsion exhibited a burst release of untrapped drug at 1 hr. The mathematical models (zero order, first order, Higuchi, and Korsmeyer-Peppas) used to evaluate the release mechanism of RIF from the nanocarrier and gel matrices suggested that the Korsmeyer-Peppas model ($r^2 > 0.99$) was the model of best fit during the first 2 hrs. Optimized cationic nanoemulsion 1 ($r^2 = 0.992$), OCNE-1 gel ($r^2 = 0.995$), and OCNE-1T gel ($r^2 = 0.993$) showed zero-order kinetics, and DS showed first-order kinetics ($r^2 = 0.997$) within the initial 2 hrs.

Ex vivo Permeation and Drug Deposition Studies

Ex vivo skin permeation and drug retention studies were performed to characterize permeation parameters following transdermal application and the effect of nanoemulsion gels on permeation behavior. The permeation enhancer Transcutol was included in one gel formulation for comparison. Permeation of RIF from DS was limited (171.98 $\mu\text{g}/\text{cm}^2$) compared to that from OCNE-1 nanoemulsion and its gel formulations at 24 hrs (Figure 8). This result was expected because RIF is lipophilic, and would not be expected to cross the SC, which consists of flattened corneocytes surrounded by lipid bilayers comprised of ceramides.⁴³

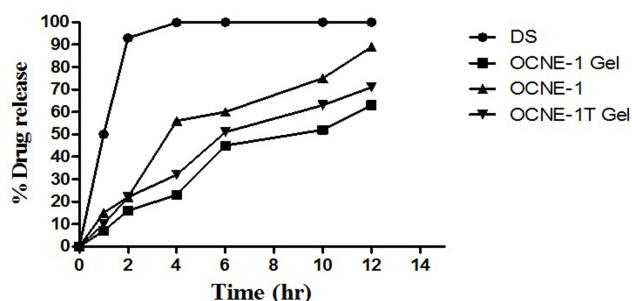


Figure 7 In vitro drug release of rifampicin from optimized formulations over a 12 hr period.

The nanoemulsion gel (OCNE-1T gel) containing Transcutol exhibited a 7.43-, 1.44- and 1.2-fold higher flux value than DS, OCNE-1, and OCNE-1 gel, respectively. The results showed that OCNE-1T gel had the highest flux value ($51.32 \pm 0.5 \mu\text{g/hr cm}^2$), which was greater than the target flux ($10.25\text{--}37.17 \mu\text{g/cm}^2 \text{ hr}$) value (Table 5). This result indicated that all of the developed nanocarriers could provide

therapeutic effects when applied transdermally, while DS could not ($7.16 \pm 0.12 \mu\text{g/hr cm}^2$). Typically applied drugs can cross the epidermis via the transcellular route, intercellular routes, and appendageal routes (hair follicles, sebaceous glands, sweat ducts). Transcellular and intercellular permeation and collectively called “transepidermal pathways.”⁴⁴ The intercellular route is the preferred pathway for lipophilic and large molecules, and may have been the route of permeation for RIF in our study.⁴⁴ Short lag time, high permeation coefficient, and augmented enhancement ratio showed that the formation of a gel and inclusion of Transcutol improved permeation (Table 5).¹⁰ The results showed that the permeation enhancer and gel carrier promoted permeation of RIF across rat skin due to increased residence time and temporary perturbation of the SC architecture.¹⁷ Thermodynamically stable nanoemulsions have been shown to enhance permeation rates and reduce lag times through synergistic interactions with the SC.^{45,46} Diffusion of RIF-loaded nanocarriers

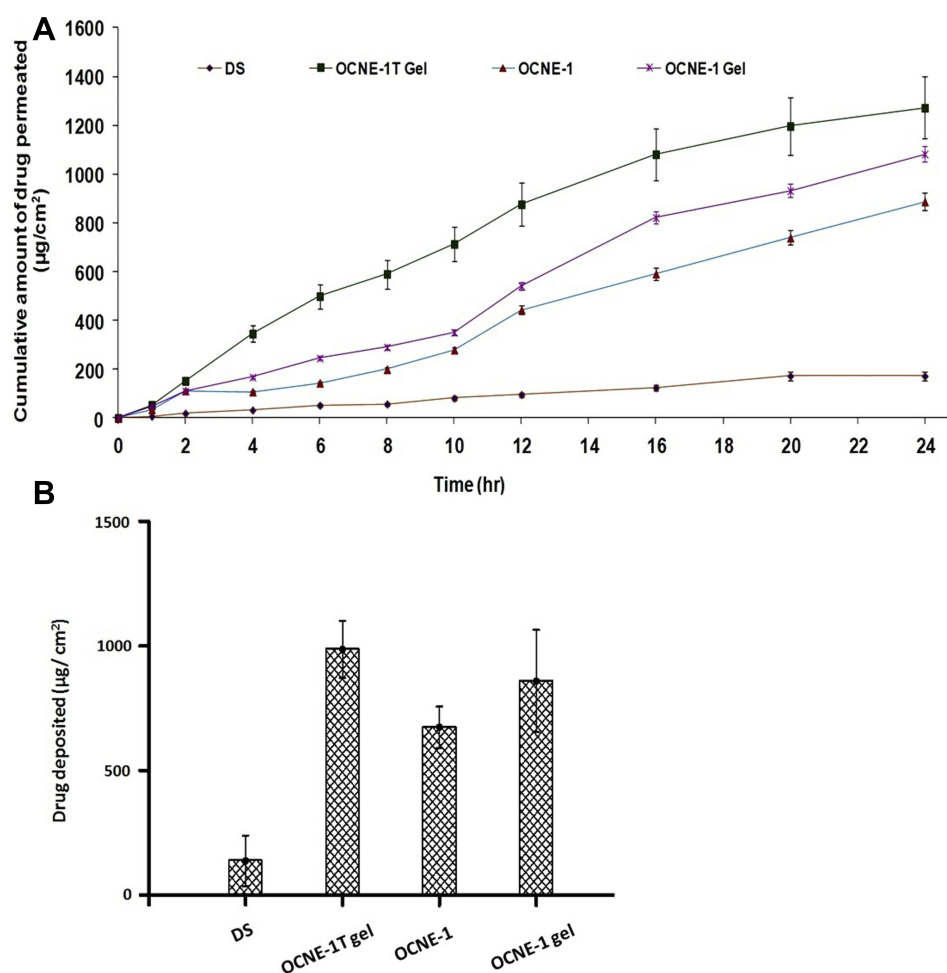


Figure 8 Ex vivo permeation and deposition studies.

Notes: (A) Ex vivo skin permeation study of optimized formulations and (B) drug deposition (retention) study of optimized formulations following transdermal application.

Table 5 Ex vivo Permeation Parameters of Rifampicin-Loaded Nanoemulsion After 24 hrs of Study

| Formulations | J_{ss}^1 ($\mu\text{g}/\text{cm}^2 \text{ hr}$) | T_L (hr) | P_c (cm/hr) | ER^2 |
|---------------|---|-----------------|------------------|--------|
| OCNE-I | 36.96 ± 1.7 | 0.58 ± 0.09 | 1.848 ± 0.03 | 5.16 |
| OCNE-I Gel | 45.09 ± 2.0 | 0.79 ± 0.10 | 2.254 ± 0.05 | 6.29 |
| OCNE-IT Gel | 51.32 ± 0.5 | 0.31 ± 0.01 | 2.566 ± 0.08 | 7.16 |
| Drug solution | 7.16 ± 0.12 | 1.1 ± 0.28 | 0.358 ± 0.01 | – |

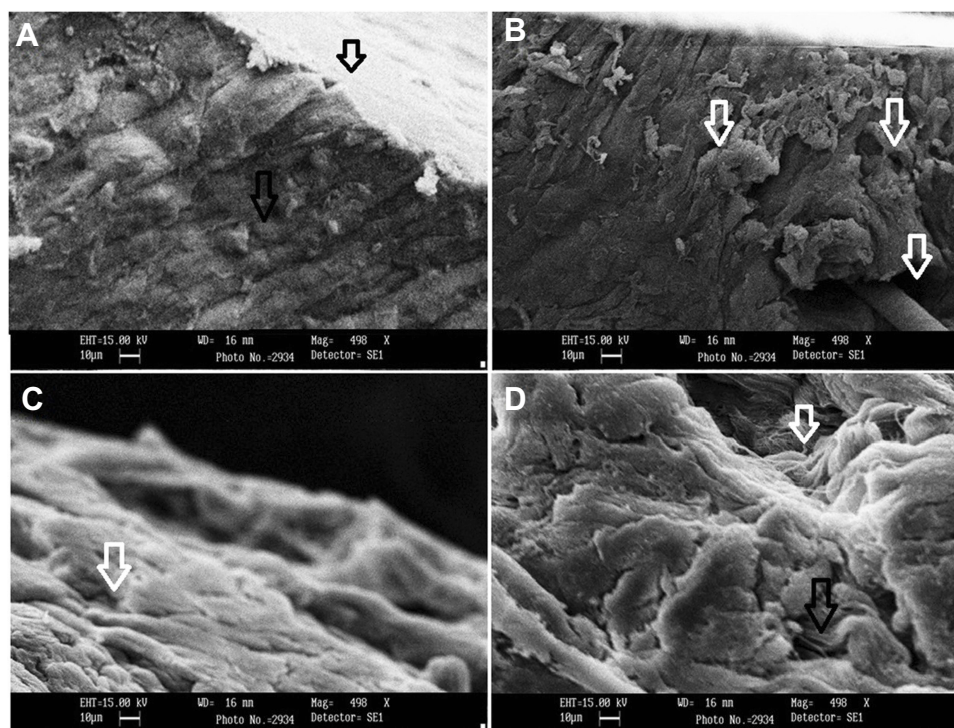
Notes: Data presented as mean \pm SD ($n = 3$). J_{ss}^1 , transdermal flux, calculated from the slope of Cartesian plot of cumulative amount of drug present in receptor compartment versus time. T_L , lag time (h). P_c , permeation coefficient = flux/the initial concentration of rifampicin dose applied to donor compartment. ER^2 , enhancement ratio; it is the ratio of transdermal flux from the formulation to drug solution (injection solution). Calculation for targeted flux = $(C_{ss} \times C_t \times BW)/\text{Area}$. Where C_{ss} = steady state concentration in plasma for rifampicin in human body (8–29 $\mu\text{g}/\text{mL}$); C_t = total body clearance (3.5 mL/min/kg = 0.058 mL/hr/kg). BW = body weight of human subject (60 kg). Area of applied site on the skin = 2.34 cm^2 .

through the SC resulted from lateral diffusion and intramembrane trans-bilayer transport.⁴⁷ Transdermal delivery of RIF using electro-phonophoresis was previously shown to slightly improve the transport of RIF across guinea pig skin.⁴¹ This showed that transdermal delivery of RIF to treat superficial tuberculosis may be a promising strategy.⁴¹ Therefore, nanoemulsion gel-based nanocarriers could be promising formulations for the treatment of local and systemic tubercular infections.

Drug localization and deposition in the skin after 24 hrs were evaluated (Figure 8B). The amounts of drug retained from OCNE-IT gel, OCNE-I gel, and OCNE-1 nanoemulsion were 994.40, 43.47, and 667.29 $\mu\text{g}/\text{cm}^2$, which were higher than that observed for DS. These values were significantly ($p < 0.05$) higher than previously reported, and were high enough to kill skin cells and promote RIF values in the circulation substantially higher than the minimum inhibitory concentration (0.25 $\mu\text{g}/\text{mL}$) of RIF.⁴¹ These results showed that RIF-loaded nanoemulsions may be promising formulations for transdermal delivery of RIF.

Ex vivo Analysis Globule–Skin Interaction Using Scanning Electron Microscopy

The optimized formulation OCNE-1 and its gels induced substantial permeation flux and drug deposition. These results were attributed to temporary and reversible changes in the SC layer that resulted in the transport of RIF to the dermal strata. Scanning electron microscopy was used to compare treated and untreated rat skin. The SC is the primary physiological barrier to the diffusion of numerous drugs. The SC is comprised of enriched flattened

**Figure 9** Scanning electron microscopy of rat skin treated with the optimized formulations.

Notes: (A) Untreated skin showing intact and normal architecture of the epidermal layer (represented with a black arrow). (B) Skin treated with OCNE-1 nanoemulsion showed significant structural changes in the upper SC layer (indicated by white arrows). (C) Skin treated with OCNE-1 gel showed perturbations in the upper SC layer (indicated by white arrows). (D) Skin treated with OCNE-IT gel showed additive perturbation of the upper SC layer by the nanoemulsion and gel that contained the permeation enhancer Transcutol (indicated by white arrows). Scale bar = 500 μm and magnification is 15,000 \times .

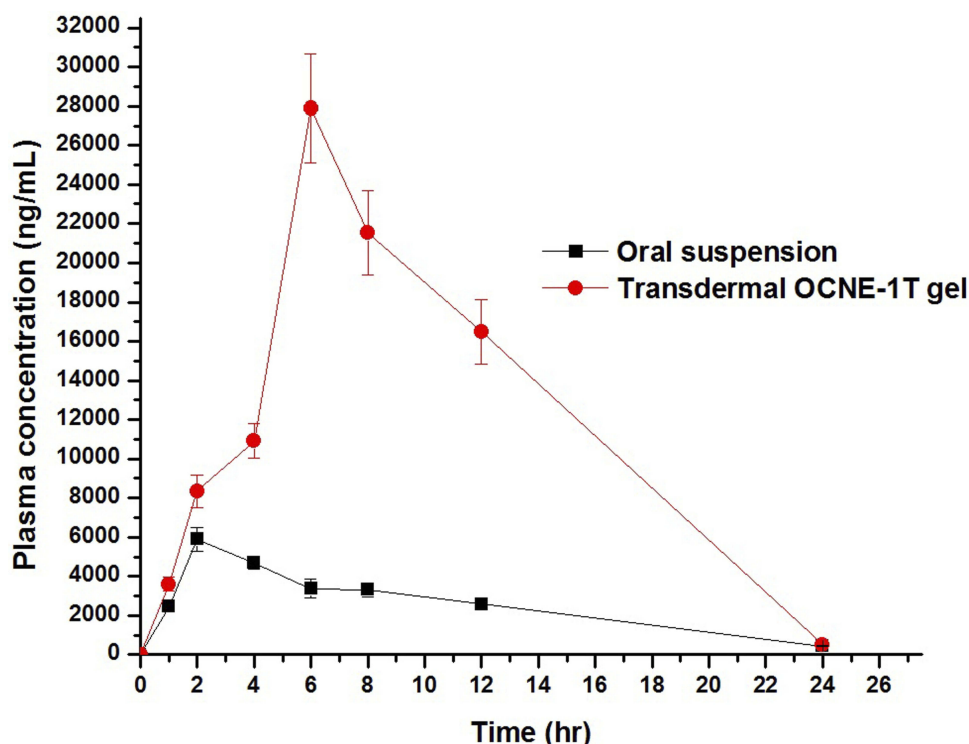


Figure 10 A comparative plasma drug concentration-time profile. Oral RIF suspension (black solid line) and transdermal RIF-loaded OCNE-1T gel (red solid line) from rat plasma.

keratinocytes and a multilamellar lipid bilayer.⁴⁸ Representative SEM images showed that untreated rat skin did not exhibit any perturbation (Figure 9A). The arrow in Figure 9A depicts the normal intact morphology of the SC layer. In contrast, the treated groups exhibited profound perturbation (white arrows show numerous fissures) and disruption on the surface, which may have been a mechanism of enhanced ex vivo transdermal permeation of the RIF nanoemulsion and its gels (Figure 9B–D). These changes in the SC may have been mediated by surfactant (S_{mix}) and CPG8.⁴⁹ The gel formulations demonstrated the ability to induce maximal reversible changes in the SC, which was optimal for transdermal delivery. These findings agreed with those from our previous report in which we showed that amphotericin B-loaded nanoemulsion gel showed enhanced permeation.⁴⁹ Baswan et al evaluated the human nail plate as a site for passive diffusion of uncharged solutes, diffusion with varied size and charge dependency of ion transport.⁵⁰ They reported that the microstructure of the nail plate is more complex than previously published findings.^{50,51} Furthermore, it is still unknown whether residual lipid barriers may impede the permeability of polar solutes.⁵¹ In addition, the absence of a permeation enhancer in the formulation could limit its penetration through the lipophilic region.⁵²

In vivo Pharmacokinetic Study

A plasma RIF concentration–time curve and PK parameters of RIF following transdermal and oral administration are shown in Figure 10 and Table 6. The calculated C_{max} and T_{max} values were 5890.0 ± 112.9 ng/mL and 2.0 hr, respectively, following the oral administration of RIF suspension. Transdermal

Table 6 Comparative Pharmacokinetic Profile of Transdermally Delivered OCNE-1T Gel and Oral RIF Suspension in Albino Rat

| PK Parameters | Oral RIF | Transdermal OCNE-1T Gel |
|--|---------------|-------------------------|
| Dose (mg) | 10 | 10 |
| C_{max} (ng mL ⁻¹) | 5890 (112.9) | 27,900 (1106) |
| T_{max} (hr) | 2.0 (0.0) | 6.0 (0.0) |
| $AUC_{(0-t)}$ μ g. hr. mL ⁻¹ | 76.31 (3.4) | 328.2 (31.6) |
| $AUC_{(0-\infty)}$ μ g. hr. mL ⁻¹ | 81.09 (4.9) | 351.9 (17.2) |
| AUMC μ g. hr ² . mL ⁻¹ | 251.86 (10.5) | 2804.6 (21.7) |
| MRT (hr) | 3.106 (0.8) | 7.97 (1.3) |
| V_d (L) | 0.382 (0.06) | 0.226 (0.25) |
| $T_{1/2}$ (hr) | 2.03 | 5.09 |
| K_{el} (hr ⁻¹) | 0.341 | 0.136 |
| F (%) | 67.93 | 89.73 |

Note: Data presented as mean (\pm standard deviation).

Abbreviations: AUC, area under curve; AUMC, area under moment curve; C_{max} , maximum plasma concentration; T_{max} , time required to reach C_{max} ; MRT, mean residence time; $T_{1/2}$, plasma half-life of drug; K_{el} , elimination rate constant; V_d , volume of distribution; F, relative bioavailability.

OCNE-1T gel resulted in C_{max} and T_{max} values of $27,900 \pm 1106$ ng/mL and 6.0 hr, respectively. Moreover, the values of $AUC_{0 \rightarrow 24}$ for oral RIF suspension and transdermal OCNE-1T gel were 76.31 ± 3.4 and 328.2 ± 31.6 $\mu\text{g hr/mL}$, respectively. These results showed that the C_{max} and $AUC_{(0-\infty)}$ for OCNE-1T gel were 4.34- and 4.74-fold higher than those for orally administered RIF suspension. Augmented skin permeation correlated with the flux value achieved in the ex vivo permeation study, which demonstrated that this may be a promising formulation for the treatment of systemic and cutaneous tuberculosis. The increase in T_{max} value from oral to transdermal administration indicated slow and sustained delivery through the skin, which was due to the viscous gel carrier and the rate-limiting nature of the SC layer. Moreover, the K_{el} (elimination rate constant) and MRT values for transdermal OCNE-1T gel were 0.136 hrs and 7.97 hr^{-1} , respectively, which were relatively higher ($p < 0.05$) than those observed following oral delivery, and were essential for prolonged action of RIF (Figure 10 and Table 6). These results showed that the developed nanoemulsion gels improved PK parameters, and may have the potential to bypass first-pass metabolism, which may allow for dose reduction and mitigation of side effects.

The result of the ex vivo and in vivo studies suggested that the developed nanoemulsion and gels improved permeation of rifampin, and may be promising transdermal delivery systems. Future studies should evaluate permeation in human skin models to gain better understanding of the clinical potential of these formulations.⁵³ Recently, poly- α -l-glutamine on the cell wall of *Mycobacterium tuberculosis* has been evaluated as a novel adjuvant with potential to improve the efficacy of human vaccines.⁵⁴ Nanoemulsions such as those developed in this study may also have potential as delivery systems for topical vaccines.

Table 7 Results of Scores Observed (Mean Value of Erythematous Scores) After Topical Application of RIF-Loaded Formulations

| Formulations | Erythematous Scores (n = 3) | | | |
|---------------------------------------|-----------------------------|--------|--------|--------|
| | 0 hr | 24 hrs | 48 hrs | 72 hrs |
| Group-I Placebo (OCNE-I nanoemulsion) | 0 | 0 | 0 | 0 |
| Group-II Placebo (OCNE-I T gel) | 0 | 0 | 0 | 0 |
| Group-III (OCNE-I nanoemulsion) | 0 | 0 | 0 | 0 |
| Group-IV (OCNE-IT gel) | 0 | 0 | 0 | 0 |
| Group-V (positive control, 5% SLS) | 0 | 3.4 | 5.2 | 3.8 |

Skin Irritation Study

None of the developed nanoemulsions caused irritation, and there were no signs of erythema for edema after 72 hrs, except in response to the positive control, sodium lauryl sulfate, which is believed to induce irritation because it is an ionic surfactant.⁵⁵ These results indicated that the cationic nanoemulsion and its corresponding gel formulations were safe, did not cause irritation, and were biocompatible. The results of this experiment are summarized in Table 7.

Conclusion

Rifampicin was efficiently administered transdermally, and CPG8 and S_{mix} were independent factors that influenced the responses (outcomes) of interest. In vitro results showed that an S_{mix} ratio of 3:1 was stable and optimal for permeation. Nanoscale globular size, increased residence time, and inclusion of Transcutol enhanced permeation across rat skin. Ex vivo results showed that Transcutol improved permeation profiles due to higher lipid extraction and reversible changes in the protein domains of the SC layers. These changes were visualized using scanning electron microscopy. Pharmacokinetic results showed that adequate plasma drug concentrations were reached following transdermal application. Transdermal delivery of rifampicin may be a promising therapeutic strategy for the treatment of systemic and cutaneous tuberculosis, and other bacterial infections.

Acknowledgment

The authors would like to thank the Deanship of Scientific Research at King Saud University for supporting this study through research group project number RG-1441-010.

Disclosure

The authors report no conflicts of interest in this work.

References

- Global Tuberculosis Report. World Health Organization (WHO); 2019. Available from: www.who.int/tb. Accessed November 30, 2019.
- Afsar FS, Afsar I, Diniz G, Asilsoy S, Sorguc Y. Lupus vulgaris in a pediatric patient: a clinicohistopathological diagnosis. *Braz J Infect Dis*. 2008;12:152–154. doi:10.1590/S1413-86702008000200011
- Puri N. A clinical and histopathological profile of patients with cutaneous tuberculosis. *Indian J Dermatol*. 2011;56:550–552. doi:10.4103/0019-5154.87153
- Thakur BK, Verma S, Hazarika D. A clinicopathological study of cutaneous tuberculosis at Dibrugarh district, Assam. *Indian J Dermatol*. 2012;57:63–65. doi:10.4103/0019-5154.92685
- Grice EA, Segre JA. The skin microbiome. *Nat Rev Microbiol*. 2011;9:244–253. doi:10.1038/nrmicro2537

6. Begum K, Shahid MS, Jalil R. Topical nanoemulsion of rifampicin with benzoic acid and salicylic acid: activity against *Staphylococcus aureus*, *Staph. epidermis* and *Candida albicans*. *Bangladesh Pharm J*. 2019;22(1):1–6. doi:10.3329/bpj.v22i1.40018
7. Begum K, Khan AF, Hana HK, Sheak J, Jalil R. Rifampicin niosome: preparations, characterizations and antibacterial activity against *Staphylococcus aureus* and *Staphylococcus epidermis* isolated from acne. *Dhaka Univ J Pharm Sci*. 2015;14:117–123. doi:10.3329/dujps.v14i1.23744
8. Wehrli W. Rifampicin: mechanism of action and resistance. *Rev Infect Dis*. 1983;5:S407–S411. doi:10.1093/clinids/5.Supplement_3.S407
9. Ahmed M, Ramadan W, Rambhu D, Shakeel F. Potential of nanoemulsions for intravenous delivery of rifampicin. *Pharmazie*. 2008;63(11):806–811.
10. Caon T, Campos CEM, Simões CMO, Silva MAS. Novel perspectives in the tuberculosis treatment: administration of isoniazid through the skin. *Int J Pharm*. 2015;494:463–470. doi:10.1016/j.ijpharm.2015.08.067
11. Prausnitz MR, Langer R. Transdermal drug delivery. *Nat Biotechnol*. 2008;26:1261–1268. doi:10.1038/nbt.1504
12. Chen S, Han Y, Yu D, et al. Transdermal delivery of isoniazid and rifampin in guinea pigs by electro-phonophoresis. *Drug Deliv*. 2017;24(1):467–470. doi:10.1080/10717544.2016.1267275
13. Aloisio C, de Oliveira AG, Longhi M. Cyclodextrin and meglumine-based microemulsions as a poorly water-soluble drug delivery system. *J Pharm Sci*. 2016;105(9):2703–2711. doi:10.1016/j.xphs.2015.11.045
14. Hussain A, Samad A, Singh SK, et al. Nanoemulsion gel-based topical delivery of an antifungal drug: in vitro activity and in vivo evaluation. *Drug Deliv*. 2016;23(2):642–647. doi:10.3109/10717544.2014.933284
15. Hussain H, Singh SK. Evidences of anti-mycobacterium activity of lipids and surfactants. *World J Microbiol Biotechnol*. 2016;32(1):1–7. doi:10.1007/s11274-015-1965-4
16. Hussain A, Singh SK, Singh N, Verma PRP. In vitro-in vivo in-silico simulation studies of anti-tubercular drugs doped with self-nanoemulsifying drug delivery system. *RSC Adv*. 2016;6:93147–93161. doi:10.1039/C6RA14122F
17. Hussain A, Singh SK, Singh N, Verma PRP. Experimental design-based optimization of lipid based self-emulsifying drug delivery system. *Pharm Dev Tech*. 2017;22(7):910–927. doi:10.1080/10837450.2016.1212879
18. Azeem A, Rizwan M, Ahmad FJ, et al. Nanoemulsion components screening and selection: a technical note. *AAPS PharmSci Tech*. 2009;10(1):69–76. doi:10.1208/s12249-008-9178-x
19. Hussain A, Singh VK, Singh OP, Shafaat K, Kumar K, Ahmad FJ. Formulation and optimization of nanoemulsion using antifungal lipid and surfactant for accentuated topical delivery of Amphotericin B. *Drug Deliv*. 2016;23(8):3101–3110. doi:10.3109/10717544.2016.1153747
20. Verma S, Kumar SK, Verma PRP, Ahsan MN. Formulation by design of felodipine loaded liquid and solid self-nanoemulsifying drug delivery systems using Box-Behnken design. *Drug Dev Ind Pharm*. 2014;40(10):1358–1370. doi:10.3109/03639045.2013.819884
21. Ong SGM, Ming LC, Lee KS, Yuen KH. Influence of the encapsulation efficiency and size of liposome on the oral bioavailability of griseofulvin loaded liposomes. *Pharmaceutics*. 2016;8(3):1–17. doi:10.3390/pharmaceutics8030025
22. Perkins WR, Minchey SR, Boni LT, et al. Amphotericin B phospholipid interactions responsible for reduced mammalian cell toxicity. *Biochim Biophys Acta*. 1992;1107:271–282. doi:10.1016/0005-2736(92)90414-H
23. Hussain A, Samad A, Singh SK, Ahsan MN, Faruk A, Ahmed FJ. Enhanced stability and permeation potential of nanoemulsion containing sefsol-218 oil for topical delivery of amphotericin B. *Drug Dev Ind Pharm*. 2014;41(5):780–790. doi:10.3109/03639045.2014.902957
24. Hussain A, Haque MW, Singh SK, Ahmed FJ. Optimized permeation enhancer for topical delivery of 5-fluorouracil-loaded elastic liposome using design expert: part II. *Drug Deliv*. 2015;23(4):1242–1253. doi:10.3109/10717544.2015.1124473
25. Skalko N, Cajkovic M, Jals'enjak I. Liposomes with metronidazole for topical use: the choice of preparation method and vehicle. *J Liposome Res*. 1998;8:283–293. doi:10.3109/08982109809035532
26. Utreja P, Jain S, Tiwary AK. Localized delivery of paclitaxel using elastic liposomes formulation development and evaluation. *Drug Deliv*. 2011;18(5):367–376. doi:10.3109/10717544.2011.558527
27. Gannu R, Palem CR, Yamsani VV, Yamsani SK, Yamsani MR. Enhanced bioavailability of lacidipine via microemulsion based transdermal gels: formulation optimization, ex vivo and in vivo characterization. *Int J Pharm*. 2010;388:231–241. doi:10.1016/j.ijpharm.2009.12.050
28. Crutcher W, Maibach HI. The effect of perfusion rate on in vitro percutaneous penetration. *J Invest Dermatol*. 1969;53:264–269. doi:10.1038/jid.1969.145
29. Hussain A, Samad A, Nazish I, Ahmed FJ. Nanocarrier-based topical drug delivery for an antifungal drug. *Drug Dev Ind Pharm*. 2013;40(4):527–541. doi:10.3109/03639045.2013.771647
30. Chen-yu G, Chun-fen Y, Qui-Lu L, et al. Development of quercetin-loaded nanostructured lipid carrier formulation for topical delivery. *Int J Pharm*. 2012;430:292–298. doi:10.1016/j.ijpharm.2012.03.042
31. Lee SH. Evaluation of acute skin irritation and phototoxicity by aqueous and ethanol fractions of *angelica keiskei*. *Exp Ther Med*. 2013;5(1):45–50. doi:10.3892/etm.2012.782
32. Vinardell MP, Mitjans M. Alternative methods for eye and skin irritation tests: an overview. *J Pharm Sci*. 2006;97:46–59. doi:10.1002/jps.21088
33. Barry III. *Mycobacterium smegmatis*: an absurd model for tuberculosis? *Trends Microbiol*. 2001;9(10):472–473. doi:10.1016/S0966-842X(01)02169-2
34. Fujiwara N, Naka T, Ogawa M, Yamamoto R, Oqura H, Taniuchi H. Characteristics of mycobacterium smegmatis J15cs strain lipids. *Tuberculosis*. 2012;92:187–192. doi:10.1016/j.tube.2011.10.001
35. Immanuel G, Sivagnanavelmurugan M, Palavesam A. Antibacterial effect of medium-chain fatty acid: caprylic acid on gnotobiotic *Artemia franciscana* nauplii against shrimp pathogens *Vibrio harveyi* and *V. Parahaemolyticus*. *Aquac Int*. 2011;19:91–101. doi:10.1007/s10499-010-9343-6
36. Singh N, Verma SM, Singh SK, Verma PRP. Antibacterial action of lipidic nanoemulsions using atomic force microscopy and scanning electron microscopy on *Escherichia coli*. *J Exp Nanosci*. 2013;10(5):381–391. doi:10.1080/17458080.2013.838702
37. Singh N, Verma SM, Singh SK, Verma PRP, Ahsan MN. Antibacterial activity of cationised and non-cationised placebo lipidic nanoemulsion using transmission electron microscopy. *J Exp Nanosci*. 2013;10(4):299–309. doi:10.1080/17458080.2013.830199
38. Singh N, Verma SM, Singh SK, Verma PRP. Consequences of lipidic nanoemulsions on membrane integrity and ultrastructural morphology of *Staphylococcus aureus*. *Mater Res Express*. 2014;1(02540):1. doi:10.1088/2053-1591/1/2/025401
39. Gonçalves JE, Fernandes MB, Chiann C, Gai MN, Souza JD, Storpirtis S. Effect of pH, mucin and bovine serum on rifampicin permeability through Caco-2 cells. *Biopharm Drug Dispos*. 2012;33:316–323. doi:10.1002/bdd.v33.6
40. Khachane PV, Jain AS, Dhawan VV, et al. Cationic nanoemulsions as potential carriers for intracellular delivery. *Saudi Pharm J*. 2015;23(2):188–194. doi:10.1016/j.jps.2014.07.007
41. Chen S, Qin M, Han Y, et al. Assessment of the efficacy of drug transdermal delivery by electro-phonophoresis in treating tuberculous lymphadenitis. *Drug Deliv*. 2016;23(5):1588–1593. doi:10.3109/10717544.2015.1124474

42. Chow KT, Chan LW, Heng PWS. Characterization of spreadability of nonaqueous 334 ethylcellulose gel matrices using dynamic contact angle. *J Pharm Sci.* 2008;97:3467–3482. doi:10.1002/jps.21227
43. Nastiti CMRR, Ponto T, Abd E, Grice JE, Benson HAE, Roberts MS. Topical nano and microemulsions for skin delivery. *Pharmaceutics.* 2017;9(4):E37. doi:10.3390/pharmaceutics9040037
44. Ng KW, Lau WM. Skin deep: the basics of human skin structure and drug penetration. In: Maibach H, editor. *Percutaneous Penetration Enhancers Chemical Methods in Penetration Enhancement: Drug Manipulation Strategies and Vehicle Effects.* Berlin/Heidelberg, Germany: Springer; 2015:3–11. ISBN 9783662450130.
45. Godwin DA, Michniak BB, Creek KE. Evaluation of transdermal penetration enhancers using a novel skin alternative. *J Pharm Sci.* 1997;86(9):1001–1005. doi:10.1021/js9700457
46. Shin SC, Choi JS. Enhanced efficacy of triprolidine by transdermal application of the EVA matrix system in rabbits and rats. *Eur J Pharm Biopharm.* 2005;61:14–19. doi:10.1016/j.ejpb.2005.03.010
47. Johnson ME, Blankschtein D, Langer R. Evaluation of solute permeation through the stratum corneum: lateral bilayer diffusion as the primary transport mechanism. *J Pharm Sci.* 1997;86:1162–1172. doi:10.1021/js960198e
48. Elias PM. The stratum corneum revisited. *J Dermatol.* 1996;23:756–758. doi:10.1111/jde.1996.23.issue-11
49. Hussain A, Singh S, Webster TJ, Ahmad FJ. New perspectives in the topical delivery of optimized amphotericin B loaded nanoemulsions using excipients with innate anti-fungal activities: a mechanistic and histopathological investigation. *Nanomedicine.* 2017;13(3):1117–1126. doi:10.1016/j.nano.2016.12.002
50. Baswan SM, Li SK, Kasting GB. Diffusion of uncharged solutes through human nail plate. *Pharm Dev Technol.* 2016;21(2):255–260. doi:10.3109/10837450.2014.991876
51. Baswan SM, Li SK, LaCount TD, Kasting GB. Size and charge dependence of ion transport in human nail plate. *J Pharm Sci.* 2016;105(3):1201–1208. doi:10.1016/j.xphs.2015.12.011
52. Baswan SM, Leverett J, Pawelek J. Clinical evaluation of the lightening effect of cytidine on hyperpigmented skin. *J Cosmet Dermatol.* 2019;18(1):278–285. doi:10.1111/jocd.2019.18.issue-1
53. Baswan S, Yim JS, Pawelek LJ. LB1591 in-vitro and in-vivo evaluation of skin lightening efficacy of cytidine. *J Investig Dermatol.* 2018;138(9):B21. doi:10.1016/j.jid.2018.06.130
54. Mani R, Gupta M, Malik A, et al. Adjuvant potential of poly- α -l-glutamine from the cell wall of *Mycobacterium tuberculosis*. *Infect Immun.* 2018;86(10):e00537–e005318. doi:10.1128/IAI.00537-18
55. Draize J, Woodard G, Calvery H. Methods for the study of irritation and toxicity of substances applied topically to the skin and mucous membranes. *J Pharmacol Exp Ther.* 1944;82:377–390.

International Journal of Nanomedicine

Dovepress

Publish your work in this journal

The International Journal of Nanomedicine is an international, peer-reviewed journal focusing on the application of nanotechnology in diagnostics, therapeutics, and drug delivery systems throughout the biomedical field. This journal is indexed on PubMed Central, MedLine, CAS, SciSearch®, Current Contents®/Clinical Medicine,

Journal Citation Reports/Science Edition, EMBase, Scopus and the Elsevier Bibliographic databases. The manuscript management system is completely online and includes a very quick and fair peer-review system, which is all easy to use. Visit <http://www.dovepress.com/testimonials.php> to read real quotes from published authors.

Submit your manuscript here: <https://www.dovepress.com/international-journal-of-nanomedicine-journal>